

Chapter 2

Concentrations of Sulfur and Nitrogen Species and Cations



Rocky Mountain National Park, Colorado (ROM206 and ROM406)

CASTNet measurements of sulfur and nitrogen air pollutants and cations were analyzed for the period 1990 through 2001. The data demonstrate a significant decline in SO_2 and sulfate concentrations. No trend is evident in the measurements of HNO_3 , nitrate, and total nitrate. NH_4^+ concentrations were slightly lower. Cation measurements show two general patterns: relatively high Na^+ levels in coastal regions and relatively high Ca^{2+} in the agricultural Midwest. CASTNet cation measurements document the appearance and transport across the United States of the Mongolian dust plume that originated in the Gobi Desert in April 2001.

CASTNet filter packs were utilized during 2001 to measure concentrations of SO_2 , SO_4^{2-} , HNO_3 , NO_3^- , total nitrate (HNO_3 plus particulate NO_3^-), NH_4^+ , and four cations – Na^+ , K^+ , Mg^{2+} , and Ca^{2+} . The presentation of the findings for each of the six primary pollutants includes a map of 2001 mean concentrations. The maps were prepared using concentration shading to illustrate the magnitude of concentrations for CASTNet sites in the continental United States.

Additionally, analyses were prepared to determine any trend in concentration for each pollutant using measurements from 34 eastern reference sites (Figure 1-1). The data from the 34 sites are presented via box plot values for each year for the period 1990 through 2001. The intersite variability among the 34 sites is shown graphically by the mean, median, and percentile values of annual mean concentrations for each year.

Finally, a map of differences between two sets of 3-year mean concentrations, 1990 through 1992 versus 1999 through 2001, was prepared for each major analyte. These two 3-year periods were selected to illustrate air quality before and after the 1995 implementation of the Phase I SO_2 emission reductions that were discussed in Chapter 1. Maps of the 2001 quarterly mean concentrations are presented in Appendix B.

The subsection on cations includes maps of 2001 mean concentrations. The sidebar at the end of the chapter (page 33) discusses the appearance and transport across the United States of the Mongolian dust plume (“the perfect dust storm”) that originated in the Gobi Desert in April 2001.

Sulfur Species

Sulfur Dioxide

A map of 2001 mean SO₂ concentrations is provided in Figure 2-1. The map shows a region of relatively high concentrations extending from southwestern Kentucky to New Jersey. This region corresponds to the major SO₂ source region shown in Figure 1-3. The highest annual SO₂ concentration levels were measured in and downwind of the Ohio River Valley with seven sites showing concentrations above 10.0 micrograms per cubic meter (µg/m³). The single highest annual mean concentration (17.3 µg/m³) at CASTNet sites in the continental United States was observed at Quaker City (QAK172) in eastern Ohio. Concentrations observed at western CASTNet sites were significantly lower than those measured in the East with only a few sites measuring levels above 1.0 µg/m³. The single highest SO₂ concentration (24.7 µg/m³) measured for any CASTNet site was observed at Hawaii Volcanoes National Park, HI (HVT424). The Kilauea Volcano produces the SO₂ concentrations measured in this national park.

Measured SO₂ concentrations are related to the geographic distribution of SO₂ emissions. The highest annual mean SO₂ concentrations were measured in and downwind of the Ohio River Valley. This region also experienced the largest decline in SO₂ concentrations over the last 12 years.

Figure 2-2 provides a box plot that illustrates the trend in annual mean SO₂ concentrations over the 12-year period 1990 through 2001. The graph shows a sharp reduction in annual mean SO₂ concentrations in 1995 in response to the Phase I emission reductions, a small increase in the median value in 1997, and a subsequent decline since then.

The difference between 3-year means from the beginning to the end of the 12-year period is 28 percent.

Changes in annual mean SO₂ concentrations for 35 eastern and six western sites are shown in Figure 2-3. The 35 eastern sites include the 34 reference sites (Figure 1-1) plus Ann Arbor, MI (ANA115). Six western sites were also included. These sites were selected because of their complete data record for the six years that were analyzed. The figure shows concentration differences by comparing two 3-year means: 1990 through 1992 and 1999 through 2001. The circles in the figure illustrate the changes (in µg/m³) from the beginning three years to the ending three years. The legend in the figure provides a scale that can be used to gauge the concentration changes, in this case, decreases. For example, the largest circle indicates a reduction of 8.0 µg/m³. In other words, the changes are directly proportional to the size of the circles. The map shows two clusters of large decreases in SO₂ concentrations – southern Illinois to southern Indiana and northern West Virginia across Pennsylvania to western New York. The single largest decrease (7.5 µg/m³) was observed at the site in Vincennes, IN (VIN140). The pattern of SO₂ concentration changes is consistent with changes in SO₂ emissions (Barnard *et al.*, 2002).

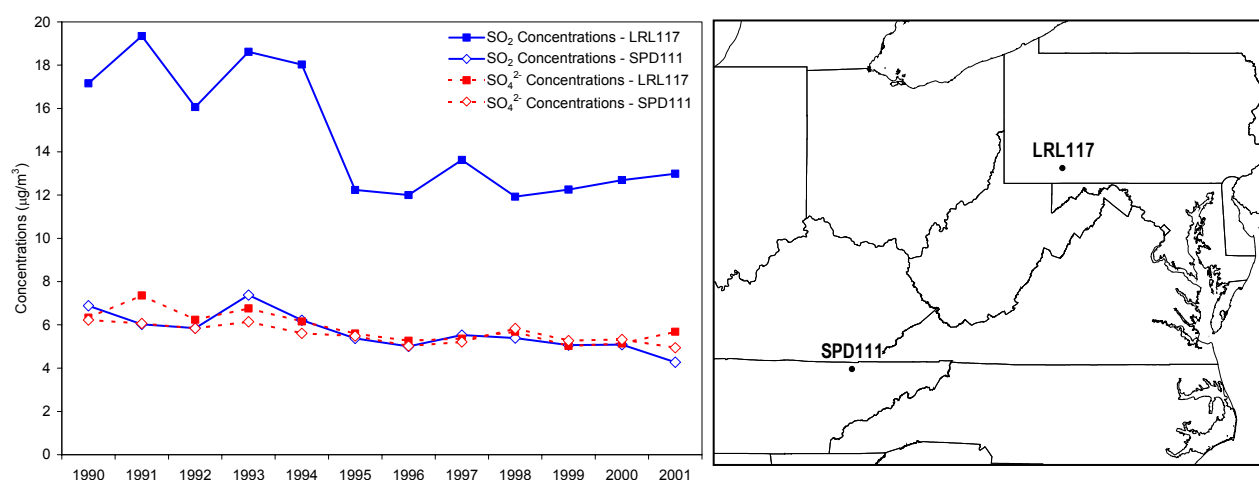
Particulate Sulfate

Annual mean particulate SO₄²⁻ concentrations observed during 2001 are presented in Figure 2-4. A large region with measured annual mean concentrations above 5.0 µg/m³ extends from Kentucky to Pennsylvania. The geographic pattern depicted by the 2001 concentrations is different from the pattern evidenced in 2000 (Harding ESE, 2002a). Higher concentrations have shifted from Alabama, Tennessee, and Kentucky to Ohio and

Trends in SO₂ and SO₄²⁻ Concentrations

Trends in highest annual mean SO₂ and SO₄²⁻ concentrations measured at two eastern sites illustrate the similarities and differences in ambient concentrations at different locations in and near the major SO₂ source region in the Ohio River Valley. Laurel Hill State Park (LRL117) is located within the source region in western Pennsylvania. Speedwell (SPD111) is located outside the source region in northeastern Tennessee, approximately 150 miles south of the Ohio River.

LRL117, the site within the source region, measured high annual mean SO₂ concentrations over the period 1990 through 2001. The differences between two sets of 3-year mean concentrations taken at the beginning and the end of this period indicate that this site experienced about a 28 percent reduction in annual mean SO₂ levels over the 12-year period. SPD111, located outside of the source region, experienced a similar decline (23 percent) in measured SO₂ concentrations even though observed concentrations were much lower.



At LRL117, annual mean concentrations of SO₂ were significantly higher than SO₄²⁻ concentrations. At SPD111, the magnitude of the SO₂ levels was about the same as that of SO₄²⁻. However, despite their vastly different locations and the difference in the magnitude of SO₂ measured at each site, annual SO₄²⁻ concentrations at the two sites were about the same. Annual mean SO₄²⁻ levels declined about 20 percent at LRL117 and approximately 14 percent at SPD111 over the 12-year period.

The data from these two sites illustrate the differences in primary and secondary pollutants and their geographic relationship to major sources. The primary pollutant SO₂ is higher in the source region whereas the secondary pollutant (particulate sulfate), which is formed from SO₂ through photochemical reactions in the atmosphere, is more uniformly distributed in and around the source region. Particulate SO₄²⁻ is produced by the accumulation of SO₂ from many sources.

Pennsylvania. In 2001, the single highest annual mean concentration of $5.9 \mu\text{g}/\text{m}^3$ was measured in eastern Ohio at QAK172. Last year, Sand Mountain, AL (SND152) recorded the highest measured annual mean concentration. The SO_4^{2-} concentration at SND152 declined from the 2000 measurement of $6.8 \mu\text{g}/\text{m}^3$ to $5.0 \mu\text{g}/\text{m}^3$ during 2001.

The trend in annual mean SO_4^{2-} concentrations is shown in the box plot in Figure 2-5. The plot shows a significant reduction in sulfate over the last 12 years. In particular, the difference between the 3-year means at the beginning and end of the 12-year period is 20 percent. This decline is less than the corresponding decline in SO_2 concentrations (see Reid *et al.*, 2001).

The region of high annual mean sulfate concentrations shifted back to the Ohio River Valley from the Deep South during 2001. However, annual mean SO_4^{2-} concentrations declined at all reference sites over the period 1990 through 2001. Sulfate concentrations have declined less rapidly than SO_2 concentrations.

Figure 2-6 illustrates changes between 3-year mean SO_4^{2-} concentrations. The legend indicates that the largest circle signifies a reduction of $2.0 \mu\text{g}/\text{m}^3$. The data show consistent decreases in ambient sulfate at all eastern and western sites. The largest decreases were observed along the Ohio River Valley from Illinois into Pennsylvania. The single largest decrease ($1.8 \mu\text{g}/\text{m}^3$) was observed at VIN140.

Nitrogen Species

Nitric Acid

A map of annual mean HNO_3 concentrations for 2001 is presented in Figure 2-7. A region in the

eastern United States with concentrations above $2.0 \mu\text{g}/\text{m}^3$ extends from western Kentucky to Connecticut. The highest annual mean concentration ($3.3 \mu\text{g}/\text{m}^3$) was measured in eastern Ohio (QAK172). Joshua Tree National Monument, CA (JOT403) measured the highest concentration ($2.5 \mu\text{g}/\text{m}^3$) in California and the West.

The box plot shown in Figure 2-8 illustrates the trend in nitric acid concentrations. The figure indicates no trend over the 12 years although the data suggest a slight decline over the last three years.

Changes between 3-year mean concentrations over the 12 years are shown in Figure 2-9. Blue circles show reductions and yellow show increases in HNO_3 concentrations. The figure displays a mixture of decreases and increases with most of the decreases observed in the northern half of the eastern sites from Illinois to Virginia northward across New England.

Particulate Nitrate

Figure 2-10 presents 2001 annual mean concentrations of particulate nitrate. The map depicts a region of relatively high levels (i.e., $2.0 \mu\text{g}/\text{m}^3$ or greater) from Wisconsin and Illinois northeastward to Ontario, Canada. The single highest value ($4.4 \mu\text{g}/\text{m}^3$) was observed in northern Illinois at Stockton (STK138). The intersite variability in the concentrations that were observed at the eastern sites is significant. For example, annual mean concentrations measured in Pennsylvania varied from 0.4 to $1.8 \mu\text{g}/\text{m}^3$. A factor of 3.0 difference was observed between concentrations measured at Georgia Station, GA (GAS153) and SND152. While most western sites measured annual mean concentrations of $0.5 \mu\text{g}/\text{m}^3$ or lower, three sites in southern California measured values above $1.0 \mu\text{g}/\text{m}^3$.

The box plot in Figure 2-11 illustrates the trend in annual mean particulate nitrate concentrations. The data show no overall trend but suggest an increase over the last three years.

Figure 2-12 shows the station-by-station changes between 3-year mean NO_3^- concentrations measured at the beginning and the end of the 12-year period. Blue circles signify decreases and yellow circles increases. The figure shows that all but four sites (Michigan, Indiana, West Virginia, and Maryland) observed higher 3-year levels at the end of the period.

Total Nitrate

Annual mean concentrations of total nitrate for 2001 are shown in Figure 2-13. The map displays a region in the eastern United States with concentrations above $4.0 \mu\text{g}/\text{m}^3$ extending from Illinois across Indiana to Ohio. The highest annual mean concentration was observed at STK138. Western CASTNet sites in southern California also measured relatively high concentrations.

Figure 2-14 provides the box plot for total nitrate values. The plot indicates no trend.

Changes between 3-year mean concentrations of total nitrate are provided in Figure 2-15. A majority of sites measured increases at the end of the 12-year period. Some sites in southeastern Michigan, Illinois, Indiana, and from Virginia northward through New England observed lower levels.

Particulate Ammonium

Figure 2-16 presents a map of 2001 annual mean particulate NH_4^+ concentrations. Sites in Illinois, Indiana, northern Kentucky, Ohio, and also Alabama observed concentrations greater than or equal to $2.0 \mu\text{g}/\text{m}^3$. With the exception of sites in Minnesota, northern New England, North Carolina, and Florida, most eastern sites measured levels above $1.0 \mu\text{g}/\text{m}^3$. Most western sites (all but four) observed annual mean NH_4^+ concentrations below $0.5 \mu\text{g}/\text{m}^3$.

Figure 2-17 presents a box plot of annual mean NH_4^+ concentrations. The data show a slight reduction in annual mean NH_4^+ concentrations over the 12-year period.

Figure 2-18 shows changes between 3-year NH_4^+ concentrations from the beginning to the end of the 12-year period. All but three reference sites measured decreases in NH_4^+ levels. The largest decreases were observed in the Midwest. Two notable increases were measured in western North Carolina.

No trend was observed in CASTNet measurements of annual mean HNO_3 , NO_3^- , and total NO_3^- concentrations, although the data suggest a decrease in HNO_3 and an increase in NO_3^- over the last three years. Ammonium measurements indicate a slight decrease over the 12 years. The nitrogen species data show considerable geographic variability with significant intersite gradients among nearby sites.

Cations

Annual mean concentrations of Na^+ , K^+ , Mg^{2+} , and Ca^{2+} for 2001 are shown in Figures 2-19 through Figure 2-22. The geographic patterns observed in 2001 are similar to those observed in 2000. Figure 2-19 shows that the highest annual mean Na^+ concentrations were observed along the coastal plain and in the South. Levels above $0.50 \mu\text{g}/\text{m}^3$ were observed from the Everglades (EVE419) in Florida to Beaufort, NC (BFT142). A single value above $0.50 \mu\text{g}/\text{m}^3$ was observed on the West Coast at Pinnacles National Monument (PIN414) in California. Concentrations above $0.20 \mu\text{g}/\text{m}^3$ were measured along both coasts. The highest annual mean Ca^{2+} concentration ($2.95 \mu\text{g}/\text{m}^3$) in the network was measured at Virgin Islands National Park (VII423). Figures 2-20 and 2-21 show relatively low annual mean measured K^+ and Mg^{2+}

concentrations and no discernible patterns. As shown in Figure 2-22, the highest annual mean Ca^{2+} concentrations were observed in the agricultural Midwest, extending from southern Illinois to Ontario, Canada. Relatively high levels were also measured along the East Coast from EVE419 to BFT142. An annual mean concentration of $0.61 \mu\text{g}/\text{m}^3$ was observed at Big Bend National Park, TX (BBE401).

The cation measurements suggest two geographic patterns. First, the highest annual mean Na^+ concentrations were in or near coastal regions from Florida to North Carolina and in California and Washington. Second, the highest annual mean Ca^{2+} concentrations were measured in the agricultural Midwest. No patterns were observed for K^+ and Mg^{2+} .

Note: In the following annual mean concentration figures, the concentration shading was prepared using an algorithm based on inverse distance cubed weighting with a radius of influence of 500 kilometers (km). Consequently, concentration estimates for areas near the geographic limits of site coverage have no meaning (e.g., western Missouri). Shading was not prepared for Alaska, Hawaii, and the Virgin Islands.

Figure 2-1. Annual Mean SO₂ Concentrations (µg/m³) for 2001

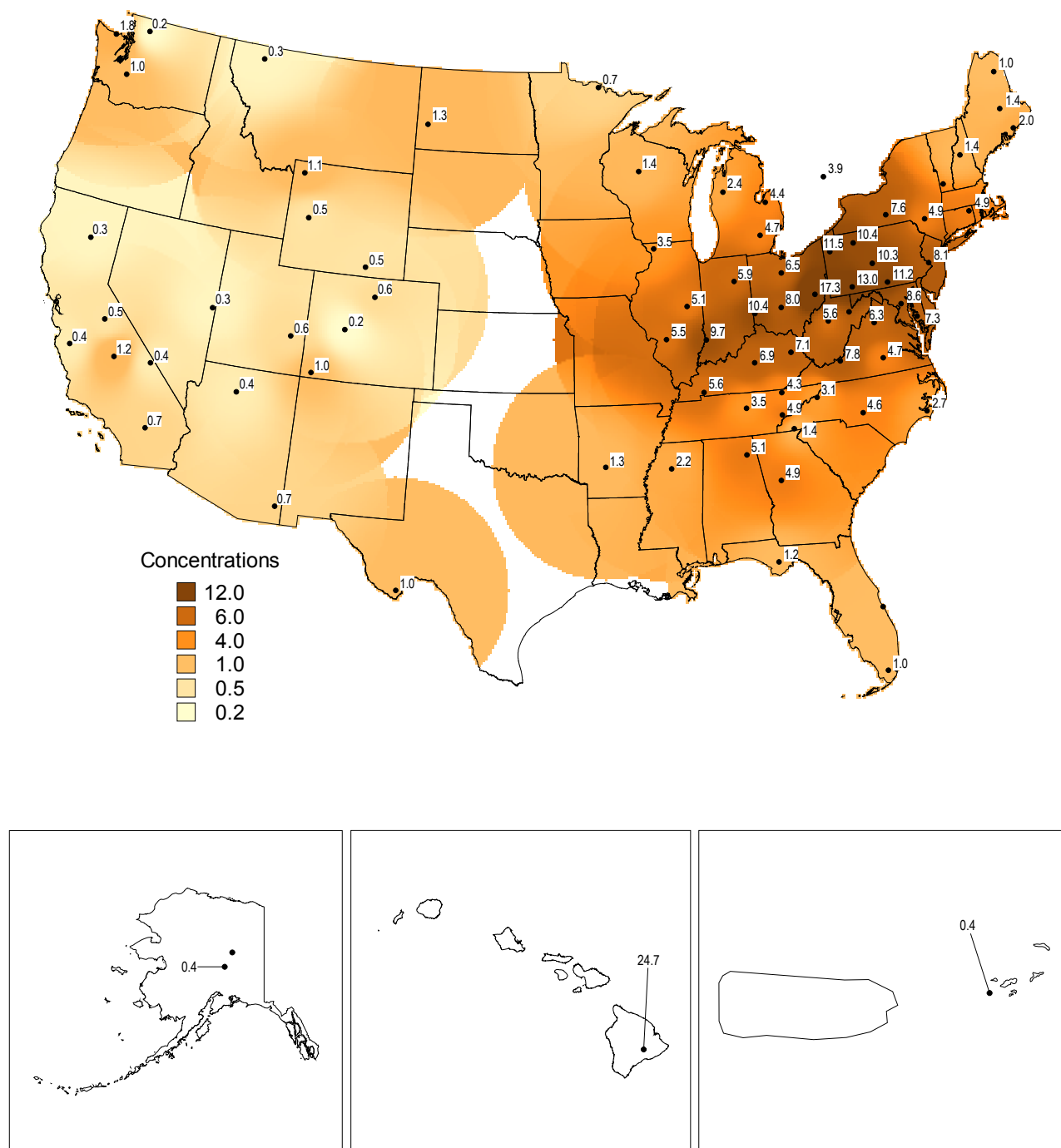


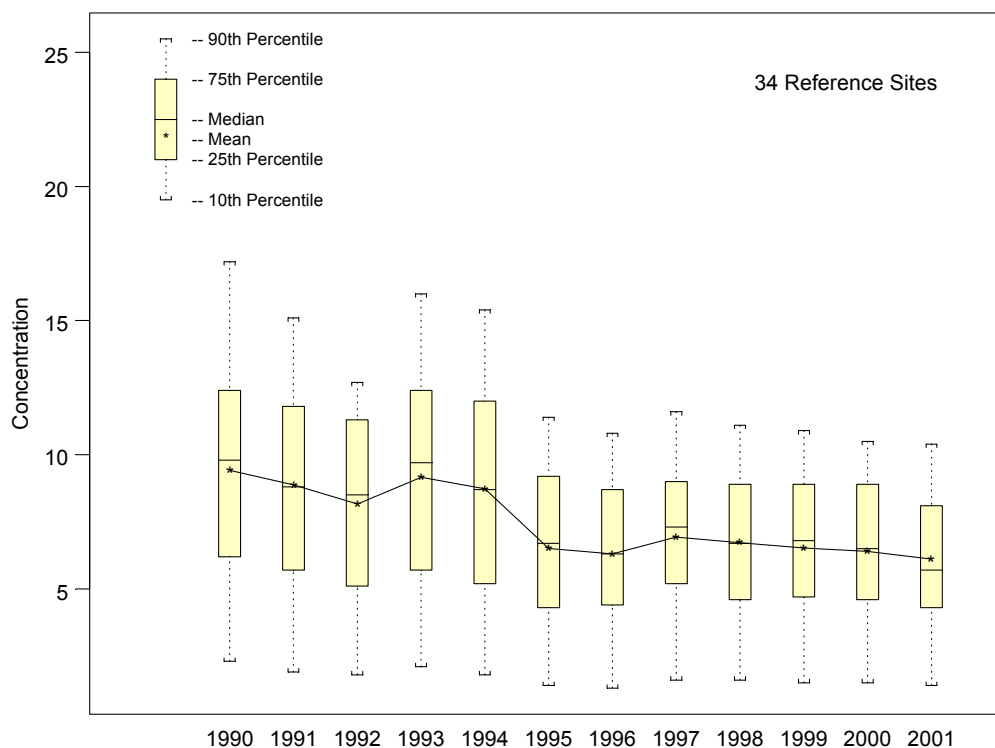
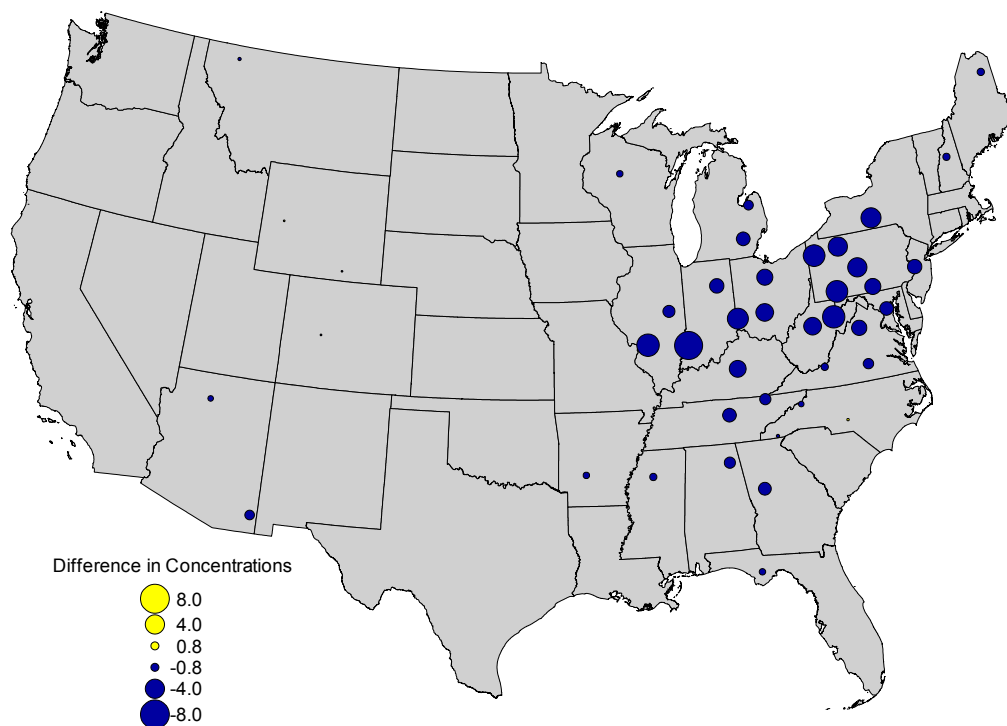
Figure 2-2. Trend in Annual SO₂ Concentrations ($\mu\text{g}/\text{m}^3$) – Eastern United States**Figure 2-3.** Differences ($\mu\text{g}/\text{m}^3$) Between 3-Year Mean SO₂ Concentrations (1990-1992 versus 1999-2001)

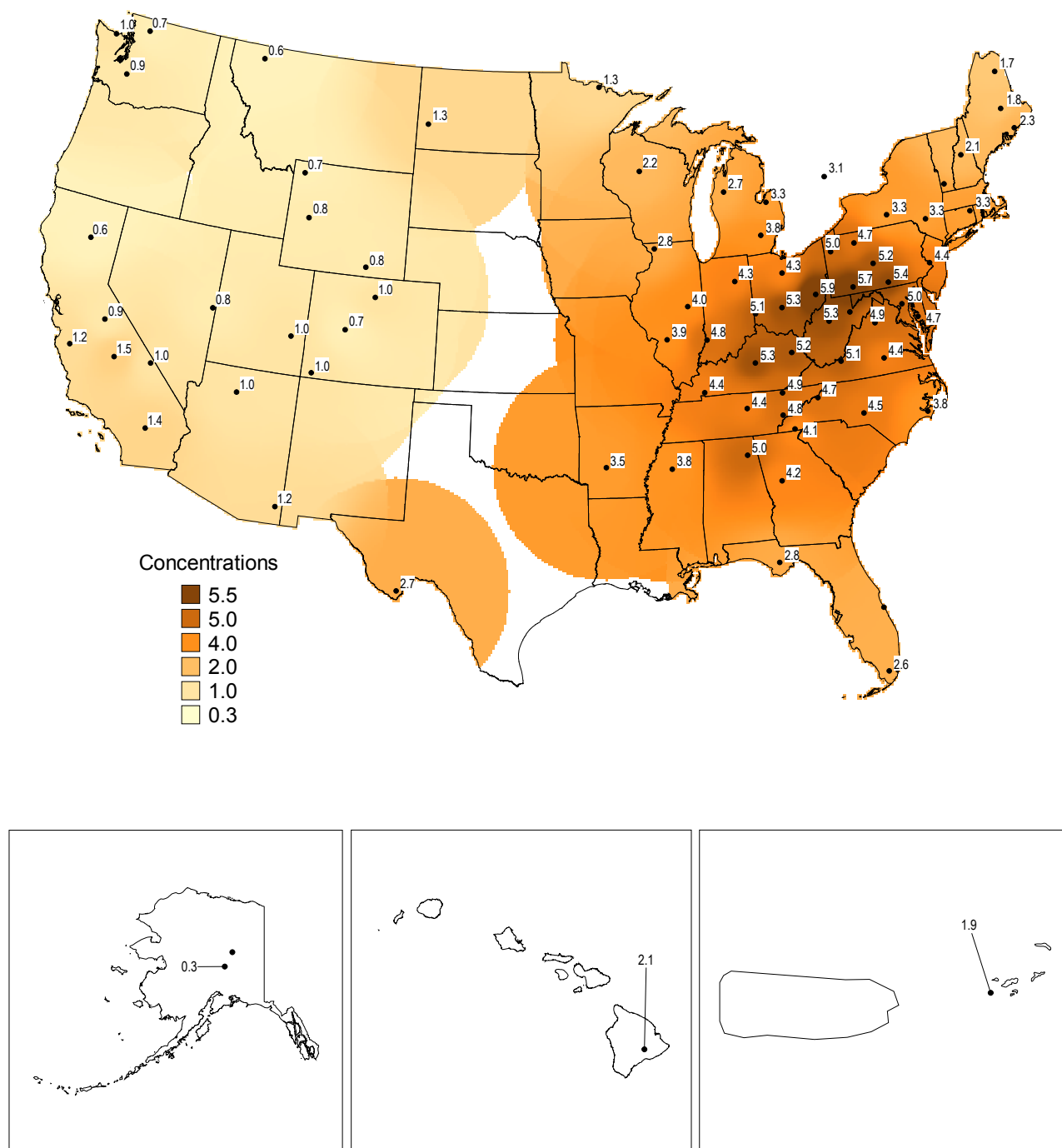
Figure 2-4. Annual Mean SO_4^{2-} Concentrations ($\mu\text{g}/\text{m}^3$) for 2001

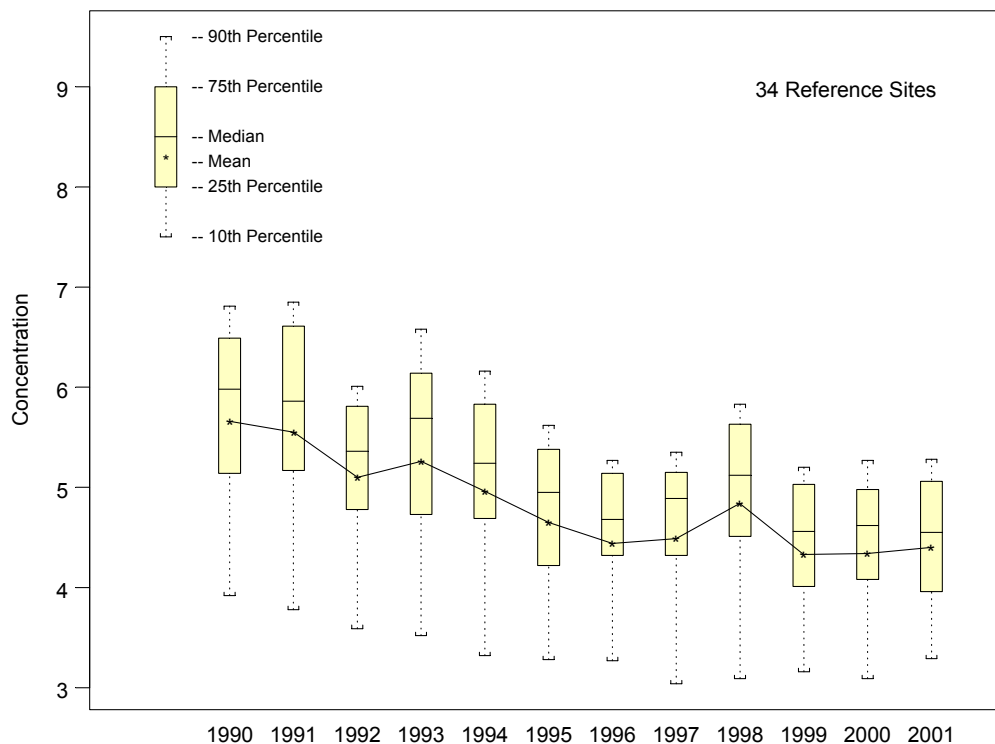
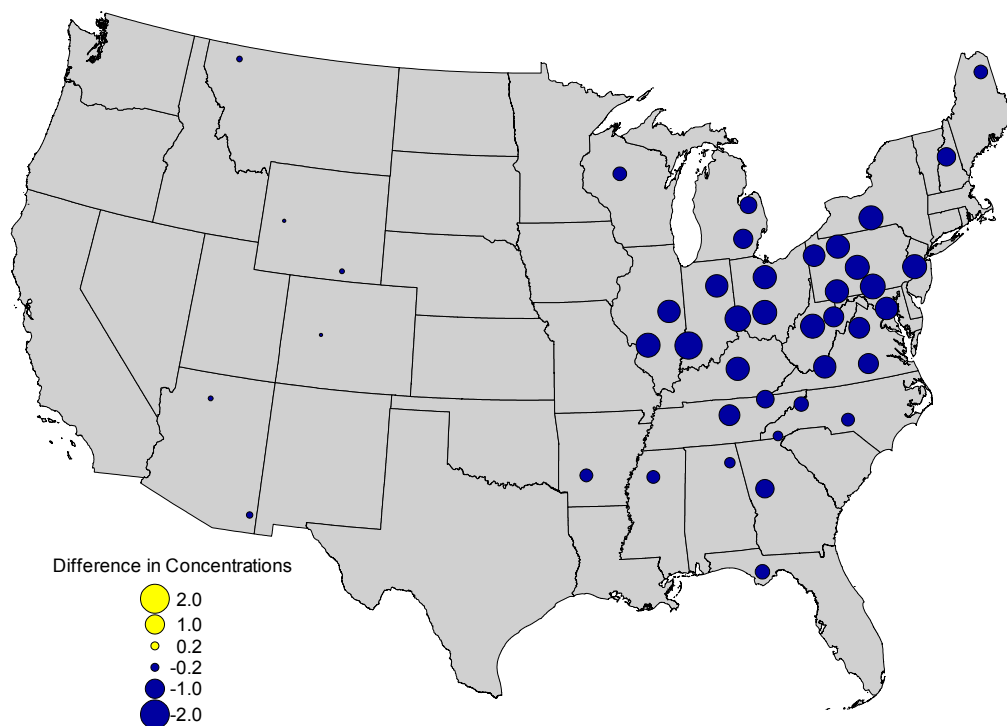
Figure 2-5. Trend in Annual SO_4^{2-} Concentrations ($\mu\text{g}/\text{m}^3$) – Eastern United States**Figure 2-6.** Differences ($\mu\text{g}/\text{m}^3$) Between 3-Year Mean SO_4^{2-} Concentrations (1990-1992 versus 1999-2001)

Figure 2-7. Annual Mean HNO_3 Concentrations ($\mu\text{g}/\text{m}^3$) for 2001

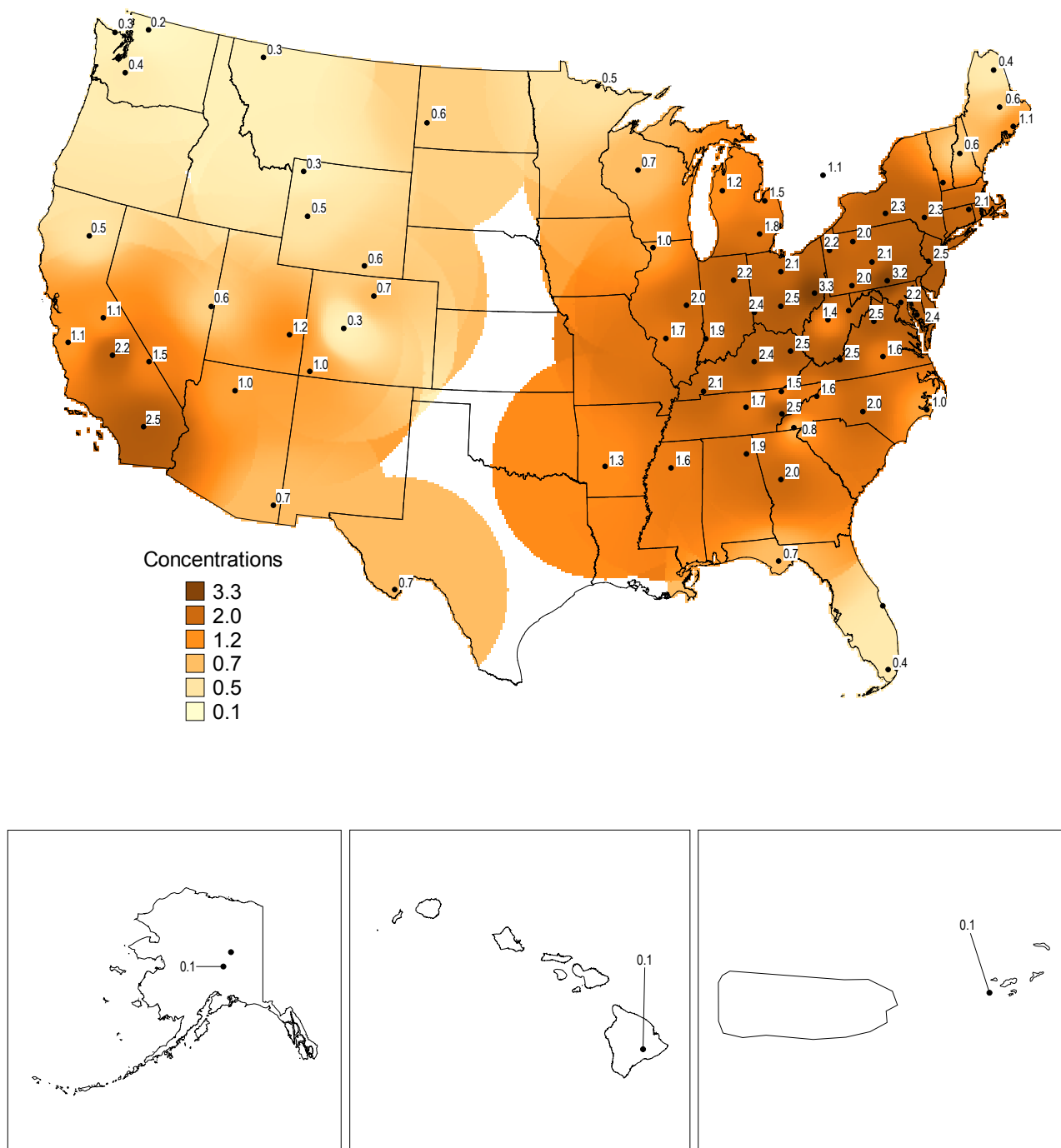


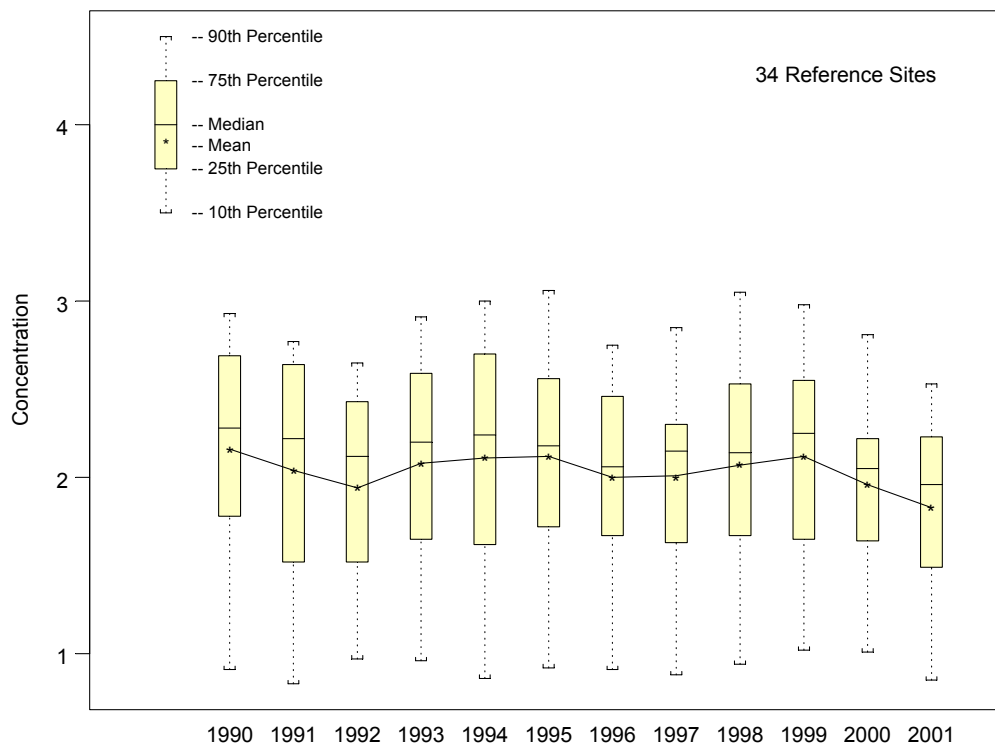
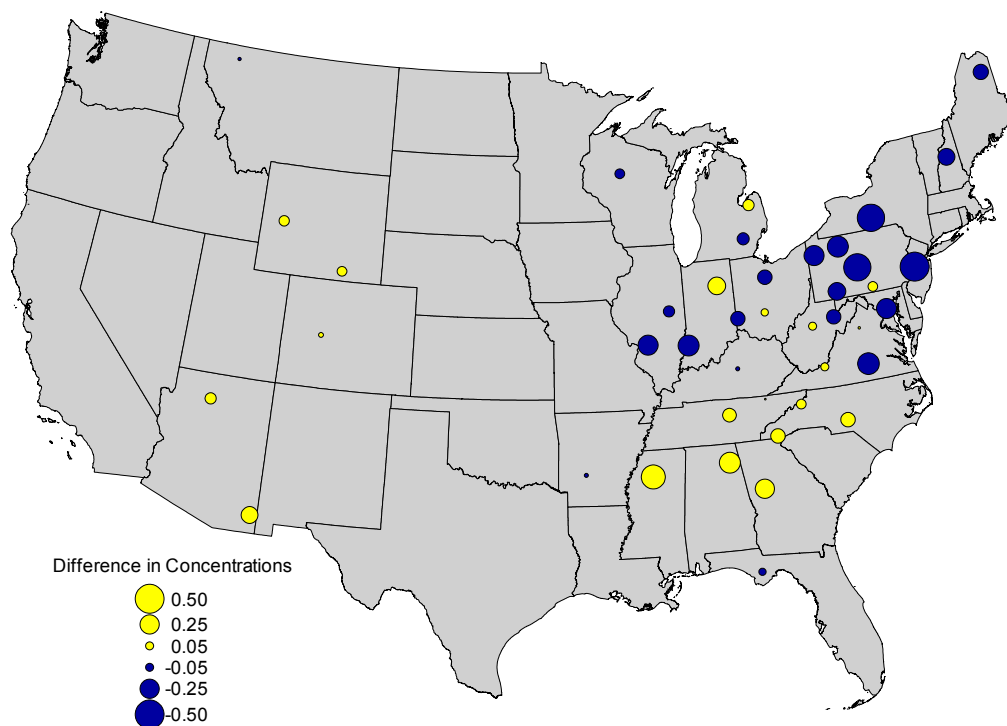
Figure 2-8. Trend in Annual HNO_3 Concentrations ($\mu\text{g}/\text{m}^3$) – Eastern United States**Figure 2-9.** Differences ($\mu\text{g}/\text{m}^3$) Between 3-Year Mean HNO_3 Concentrations (1990-1992 versus 1999-2001)

Figure 2-10. Annual Mean NO_3^- Concentrations ($\mu\text{g}/\text{m}^3$) for 2001

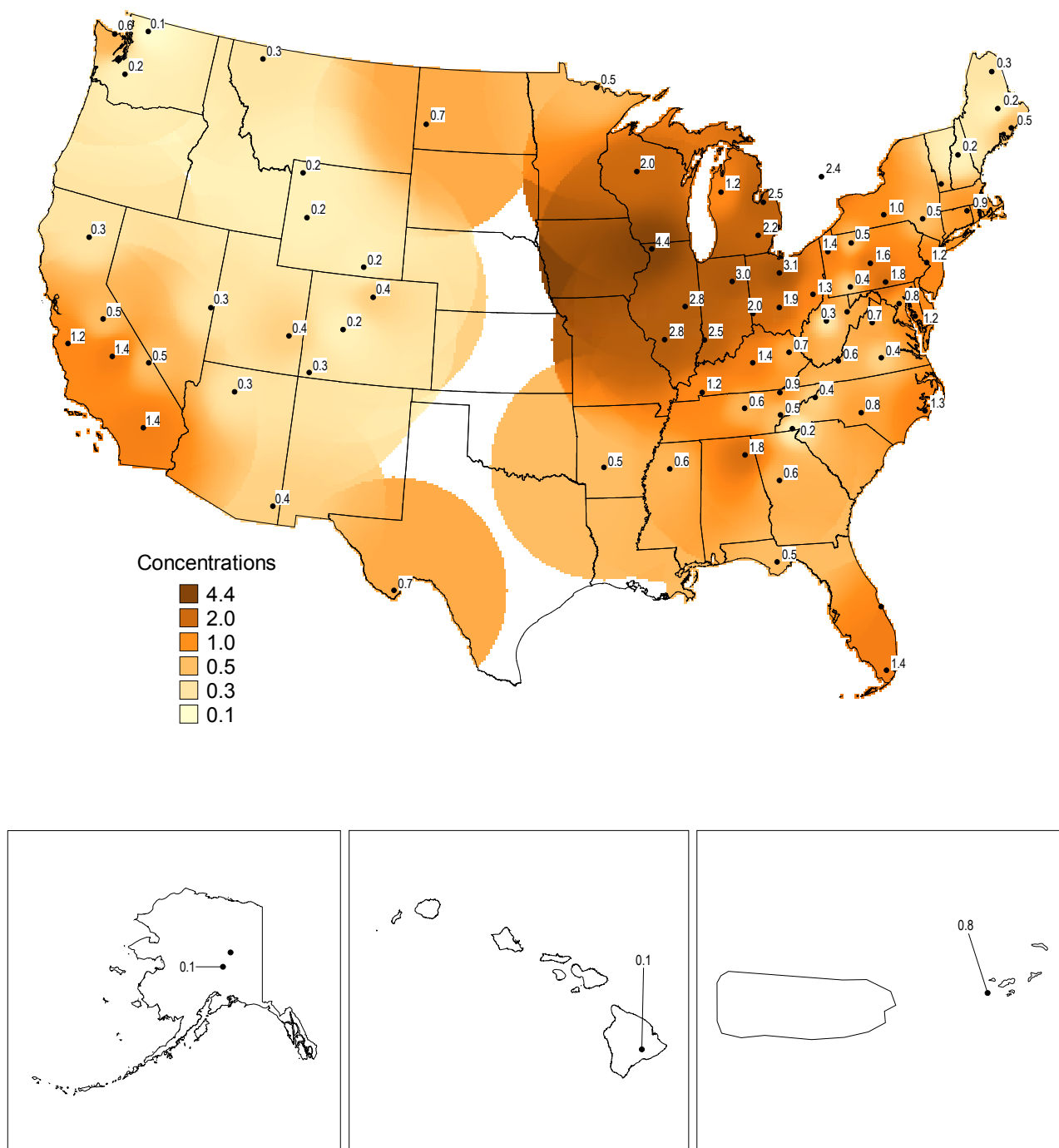


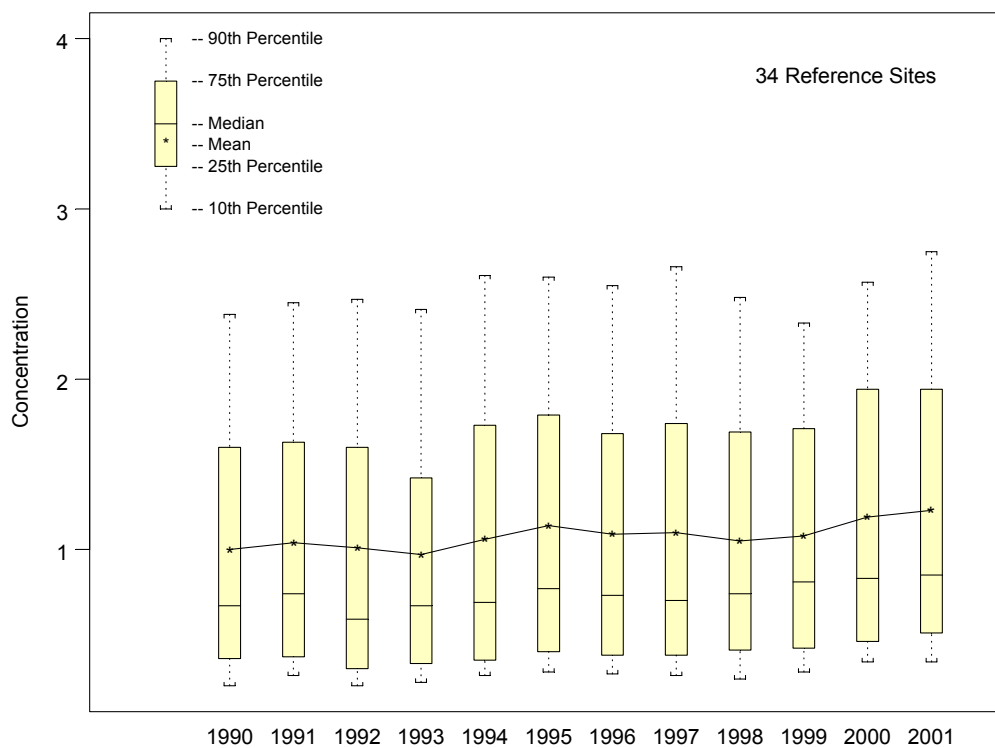
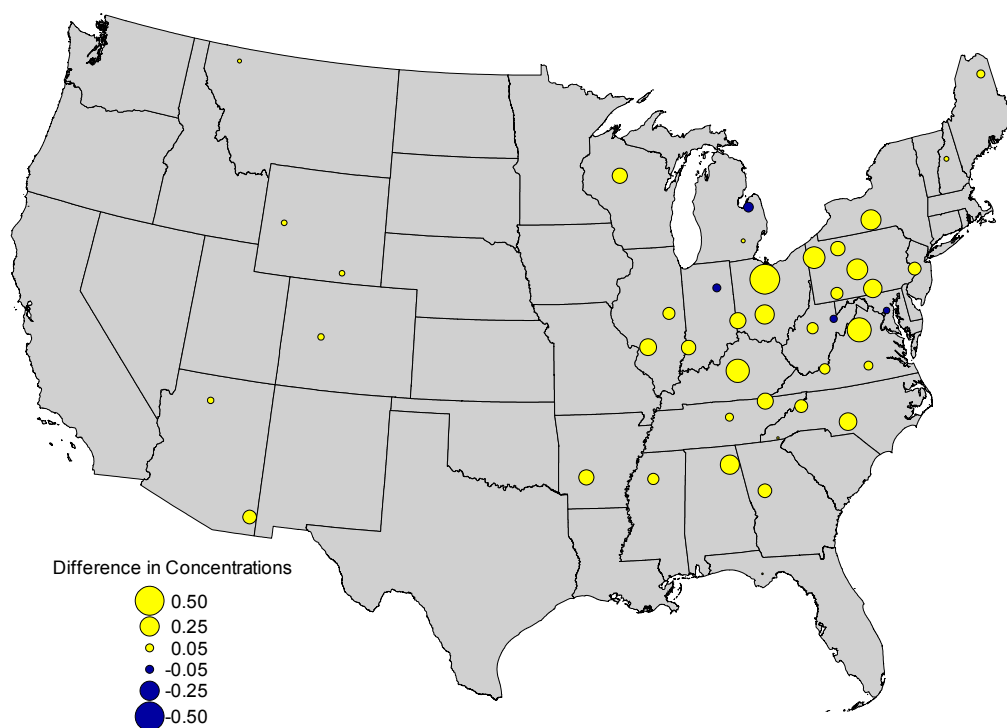
Figure 2-11. Trend in Annual NO_3^- Concentrations ($\mu\text{g}/\text{m}^3$) – Eastern United States**Figure 2-12.** Differences ($\mu\text{g}/\text{m}^3$) Between 3-Year Mean NO_3^- Concentrations (1990-1992 versus 1999-2001)

Figure 2-13. Annual Mean Total NO_3^- Concentrations ($\mu\text{g}/\text{m}^3$) for 2001

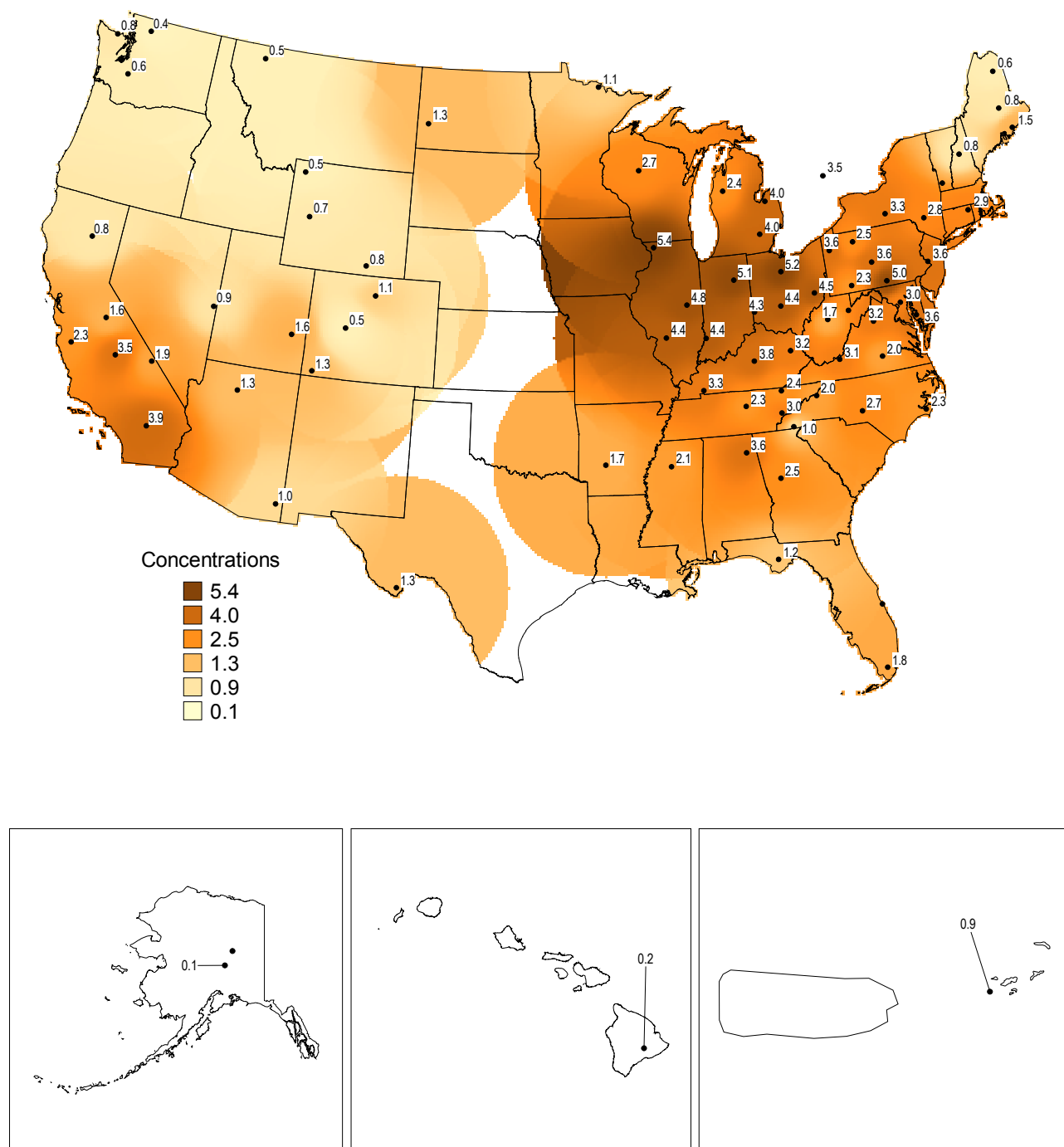


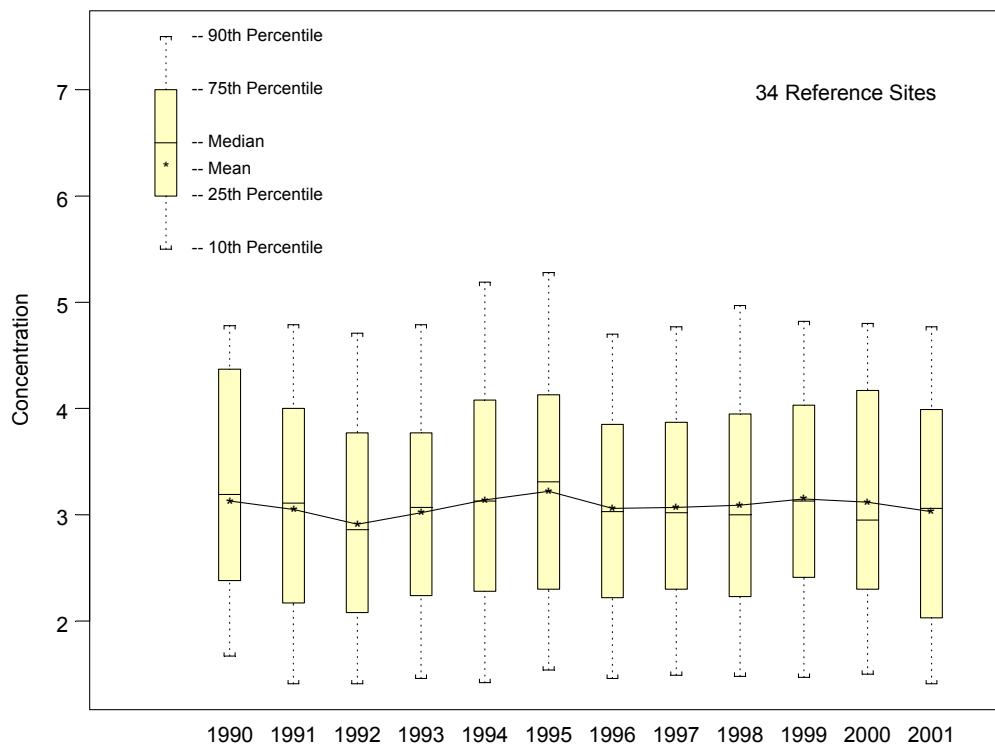
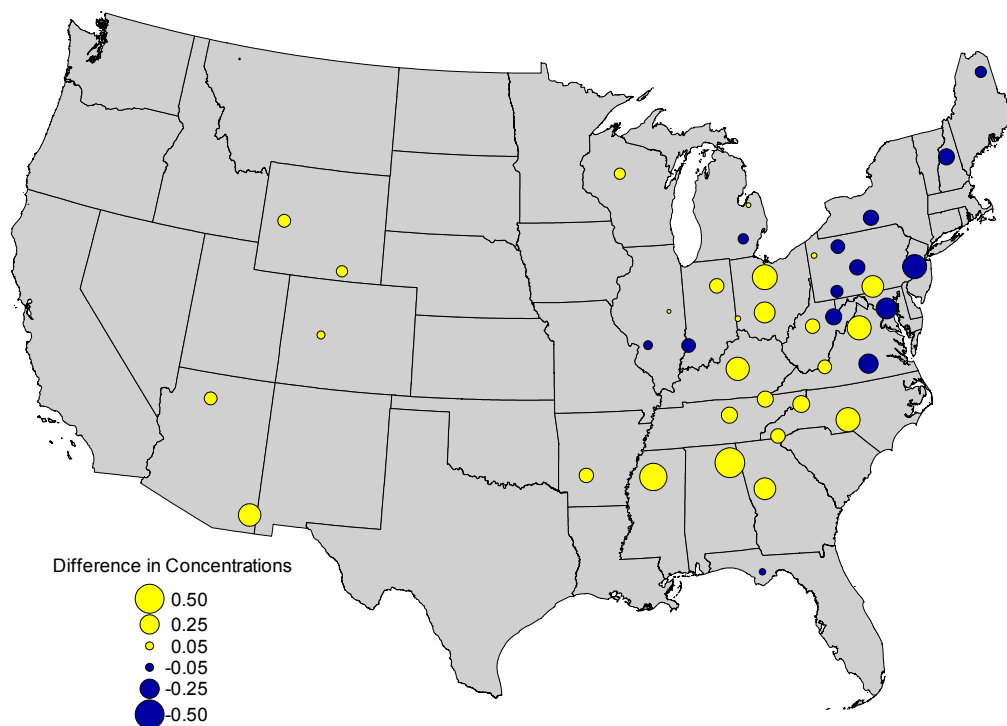
Figure 2-14. Trend in Annual Total NO_3^- Concentrations ($\mu\text{g}/\text{m}^3$) – Eastern United States**Figure 2-15.** Differences ($\mu\text{g}/\text{m}^3$) Between 3-Year Mean Total NO_3^- Concentrations (1990-1992 versus 1999-2001)

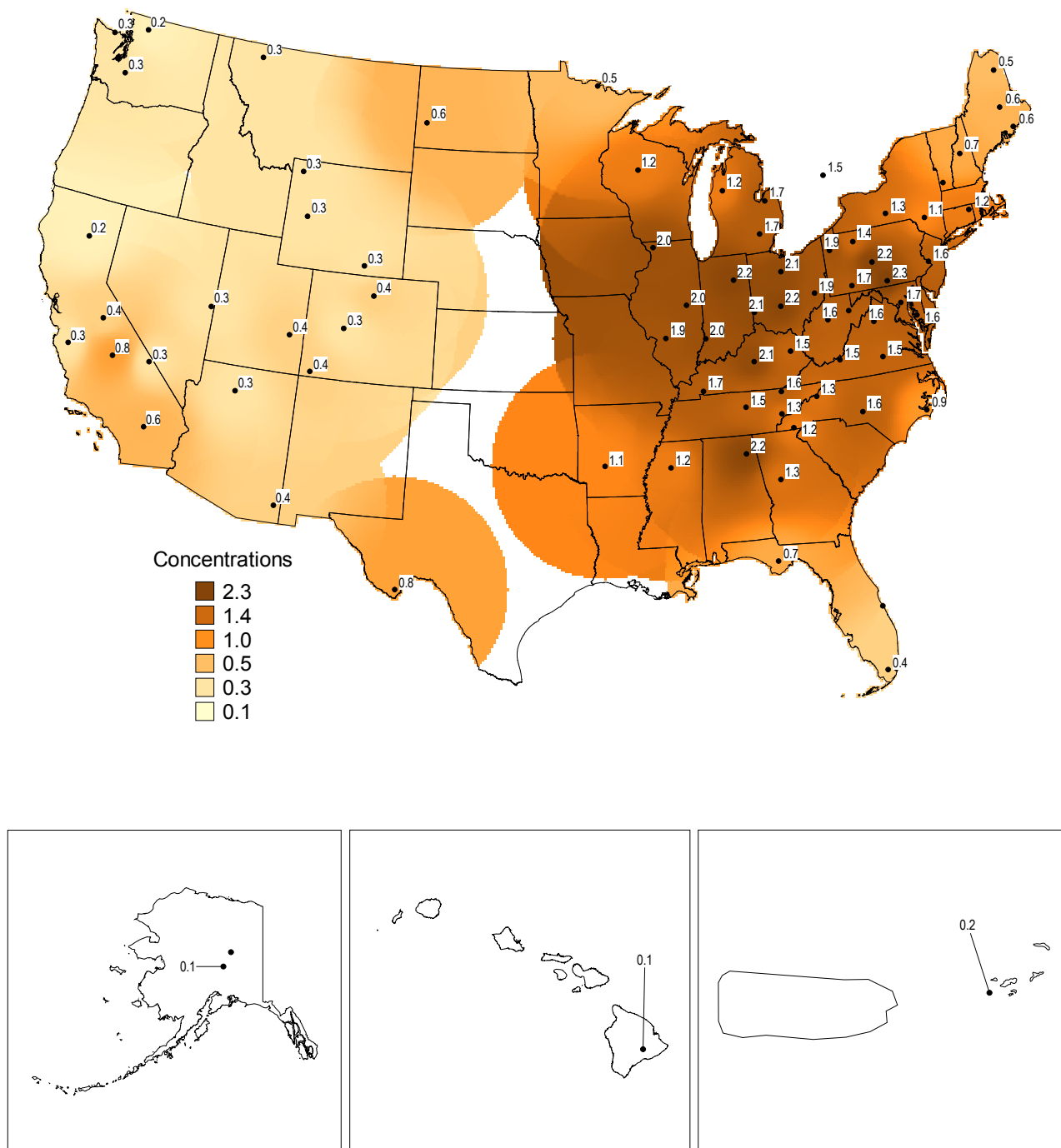
Figure 2-16. Annual Mean NH_4^+ Concentrations ($\mu\text{g}/\text{m}^3$) for 2001

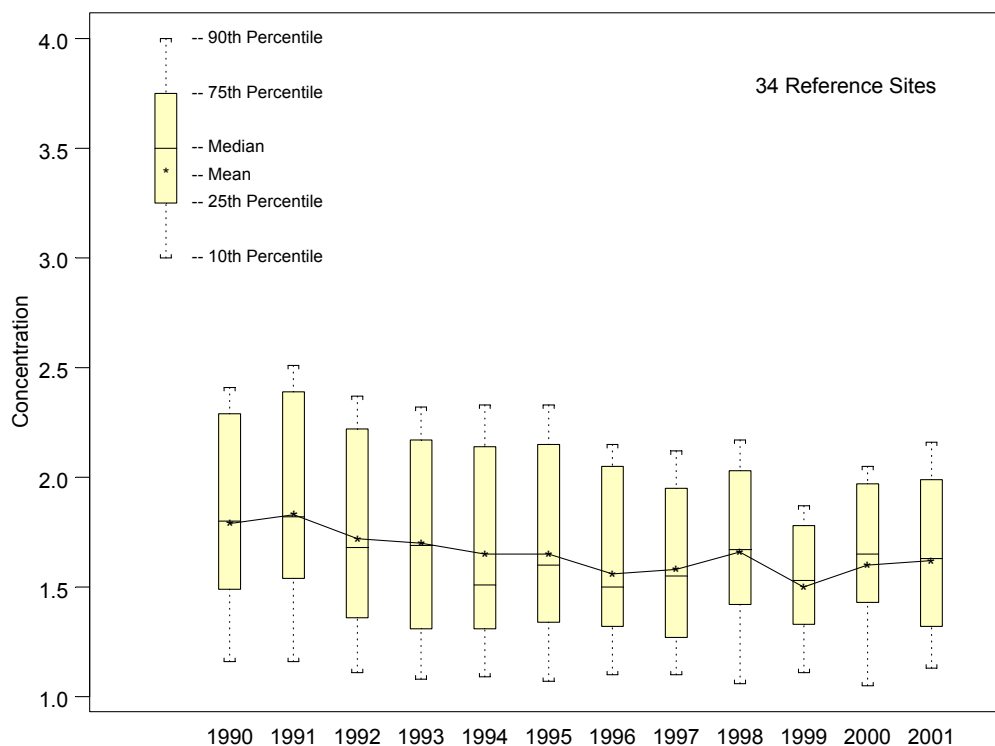
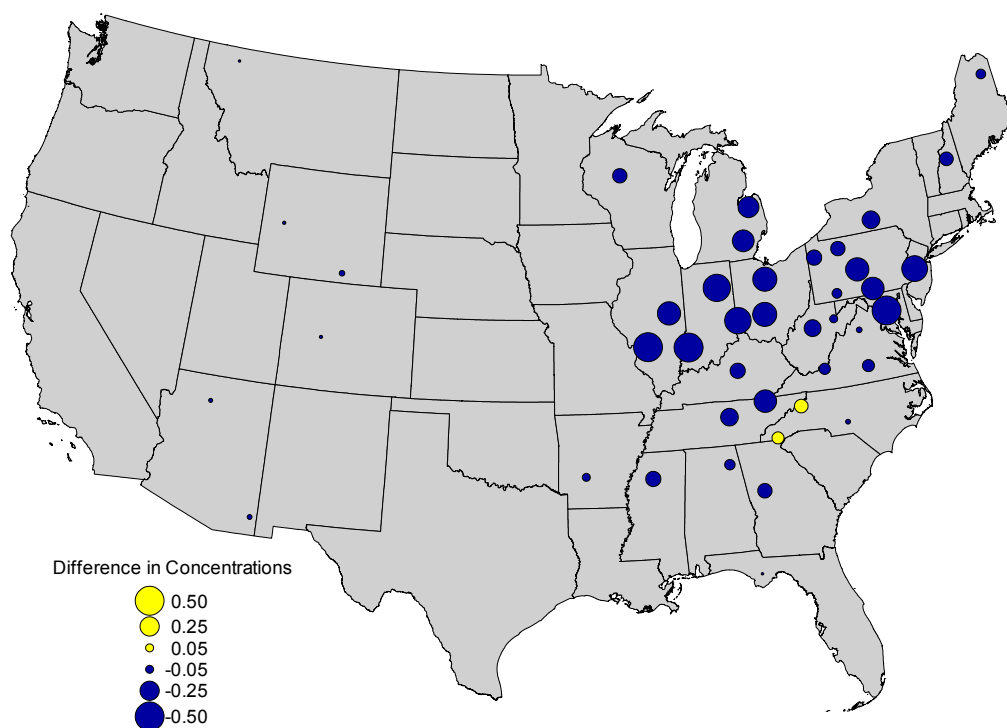
Figure 2-17. Trend in Annual NH_4^+ Concentrations ($\mu\text{g}/\text{m}^3$) – Eastern United States**Figure 2-18.** Differences ($\mu\text{g}/\text{m}^3$) Between 3-Year Mean NH_4^+ Concentrations (1990-1992 versus 1999-2001)

Figure 2-19. Annual Mean Na^+ Concentrations ($\mu\text{g}/\text{m}^3$) for 2001

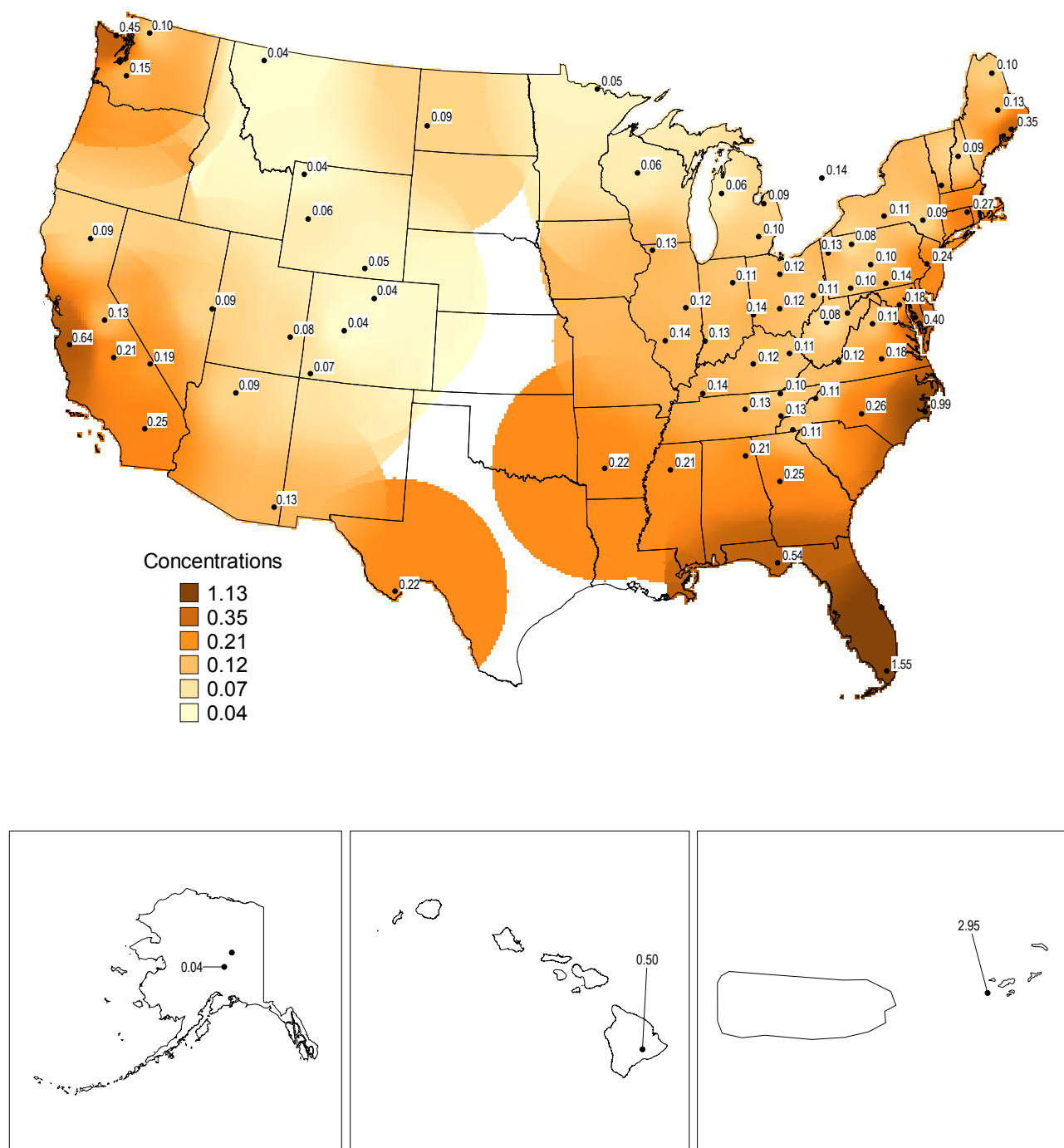


Figure 2-20. Annual Mean K^+ Concentrations ($\mu\text{g}/\text{m}^3$) for 2001

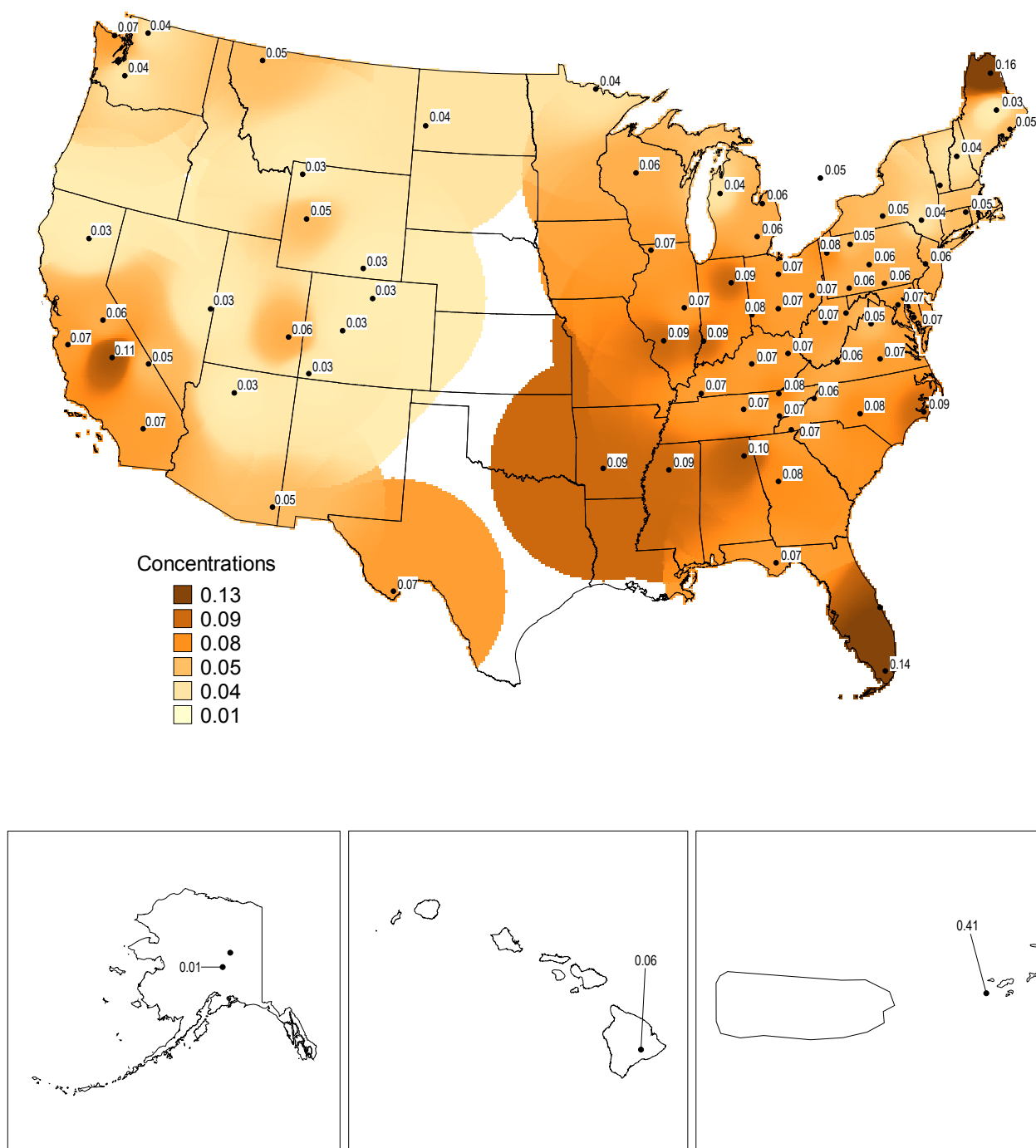


Figure 2-21. Annual Mean Mg^{2+} Concentrations ($\mu\text{g}/\text{m}^3$) for 2001

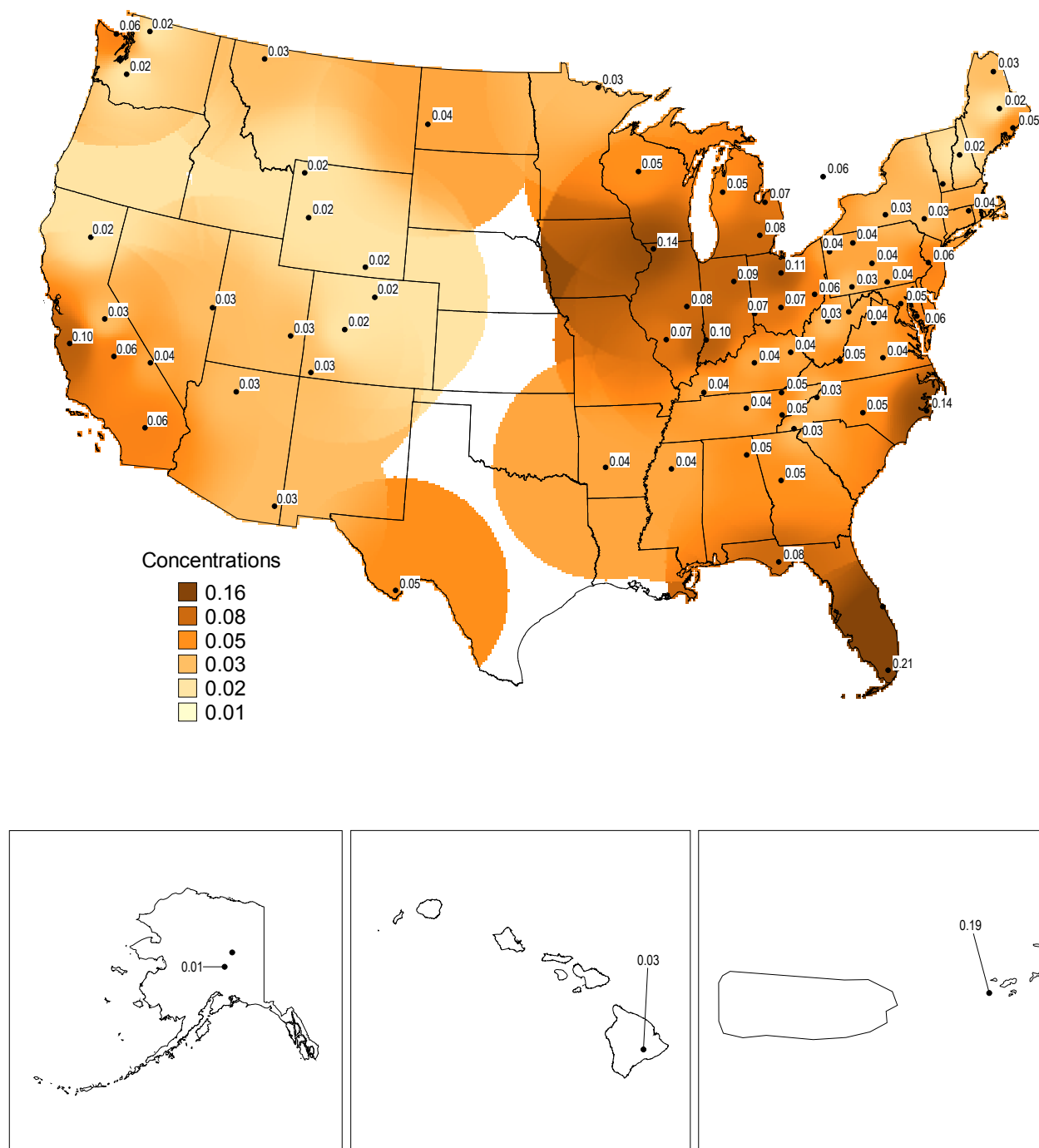
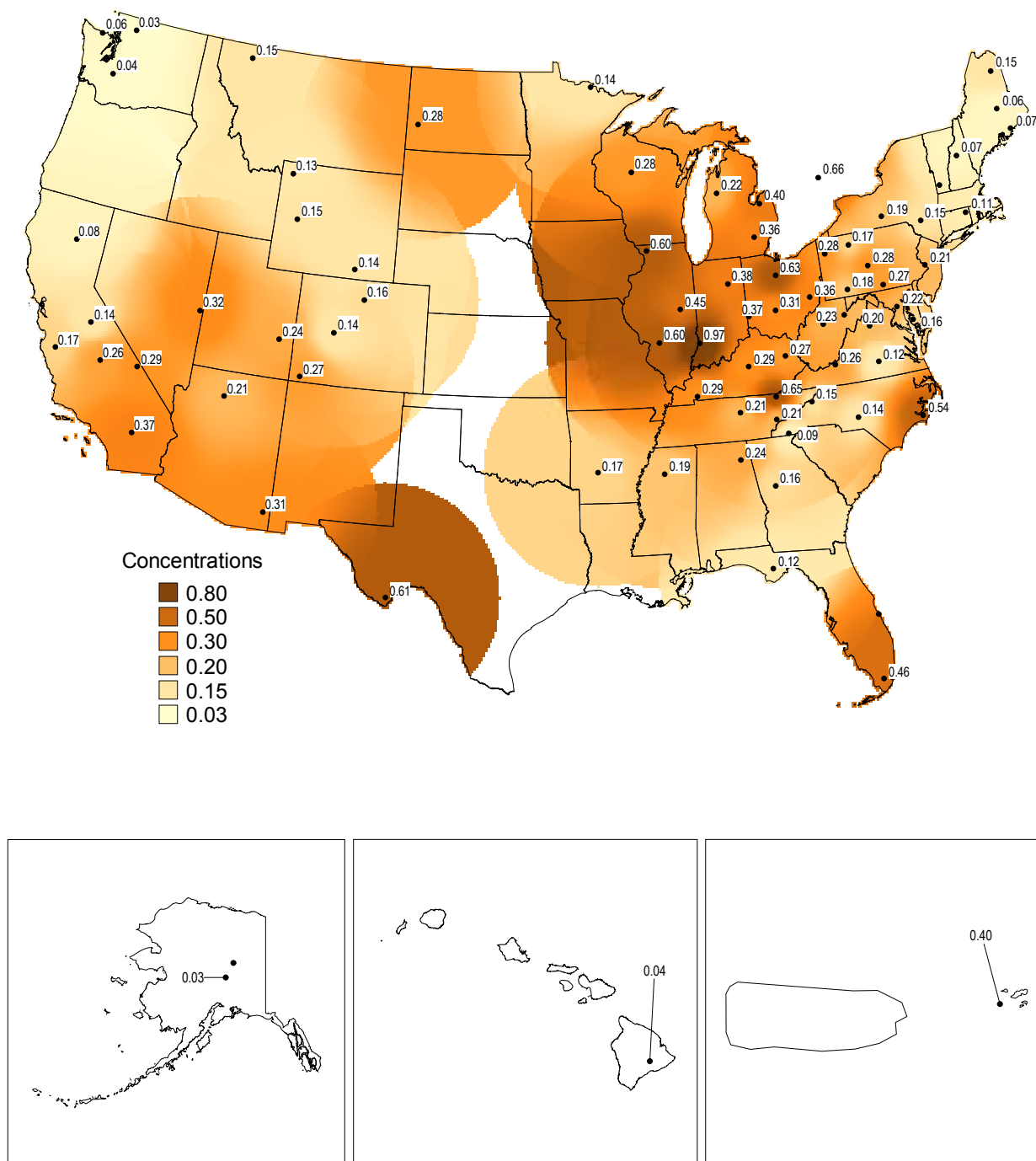


Figure 2-22. Annual Mean Ca^{2+} ($\mu\text{g}/\text{m}^3$) Concentrations for 2001



This page intentionally left blank.

The Perfect Dust Storm

The CASTNet cation measurements document the appearance and transport across the United States of the Mongolian dust plume that originated in the Gobi Desert in April 2001 (NOAA, 2001; NASA, 2001). NASA scientists have called the event the “perfect Asian dust storm.” D. Jaffe and his colleagues have shown that Asian emissions are frequently transported to North America during spring and contribute significantly to atmospheric pollutant concentrations (1999). The April 2001 dust storm is an example of these spring transport events. Satellite data from the Earth Probe Total Ozone Mapping Spectrometer (TOMS) aerosol index (Herman *et al.*, 1997) show the eruption of dust in East Asia on April 7, 2001 (Figure 2-i). Subsequent TOMS data (Figures 2-ii through 2-v) illustrate the transport of the dust cloud across the Pacific and the United States and its subsequent dilution and break-up.

Time series of weekly Ca^{2+} , K^+ , and Mg^{2+} concentrations were constructed from measurements taken at sites located across the United States. Time series that track the concentrations measured in California (LAV410), Colorado (GTH161), Arkansas (CAD150), Virginia (PED108), and North Carolina (BFT142), are shown in Figures 2-vi through 2-viii. These figures illustrate the movement of the dust across the United States. The time series show evidence of the plume entering the western United States during the week of April 10, 2001. For example, weekly Ca^{2+} concentrations from the westernmost sites (LAV410, GTH161, and CAD150) reached their maximum during the week of April 10, 2001. Calcium concentrations measured at the next site in the path of the plume’s eastern progression, PED108, peaked during the following week. Levels at BFT142, the easternmost site, peaked during the week of April 24, 2001. Similar results are evident from the time series of K^+ and Mg^{2+} concentrations shown in Figures 2-vii and 2-viii, although the graphs show more “noise.”

Maps of weekly Ca^{2+} concentrations for the four weeks beginning April 3, 2001 are shown in Figures 2-ix through 2-xii. The presence of the dust cloud is not evident during the first week (4/3/01). Concentration values observed during that week were typical of annual means. Ca^{2+} concentrations indicated the presence of the dust cloud crossing the United States during the week of April 10, 2001. Concentration levels at CASTNet sites in California and the Rocky Mountains were three to five times higher than the annual means. On the other hand, the maps provide no indication of significant Ca^{2+} concentrations in Washington despite the presence of the dust cloud in the region per the TOMS images (Figure 2-ii). Perhaps the dust had remained in the free troposphere over Washington and was not dispersed to ground level until the cloud experienced significant vertical turbulent mixing over the continental United States (Jaffe *et al.*, 1999). The CAD150 data suggest the cloud reached Arkansas by the end of the week. The Ca^{2+} concentrations observed during the week of April 17, 2001 illustrate that the cloud reached the eastern United States, as shown by the atypically high concentrations observed in New England southward to Florida. The Ca^{2+} data for the week of April 24, 2001 indicate that the dust lingered along the East Coast. According to the measurements depicted in the time series graphs, the Ca^{2+} concentrations returned to “normal” levels by mid-May.

Figure 2-i. TOMS Aerosol Index for April 7, 2001

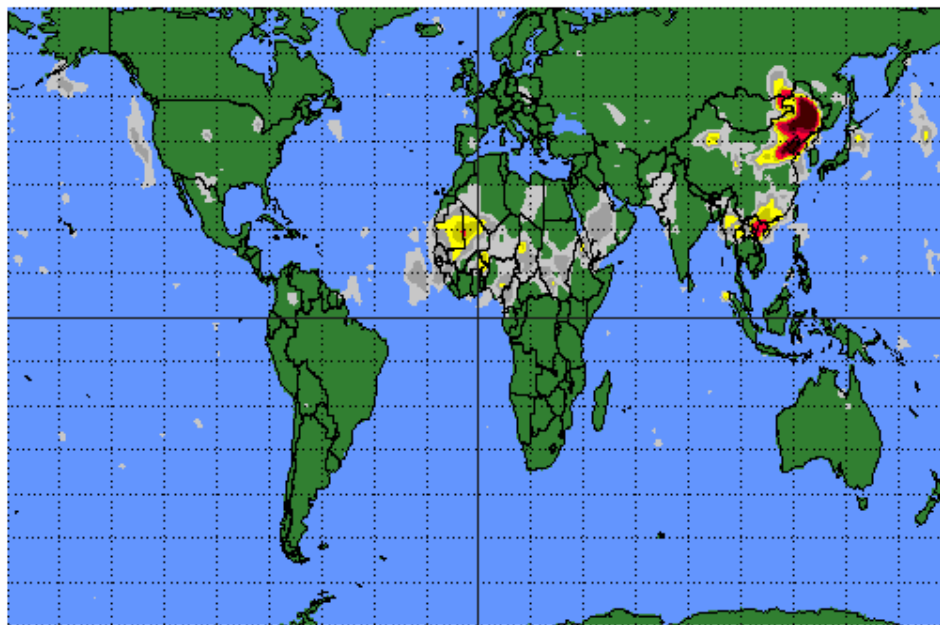
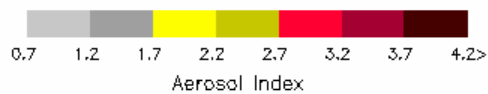
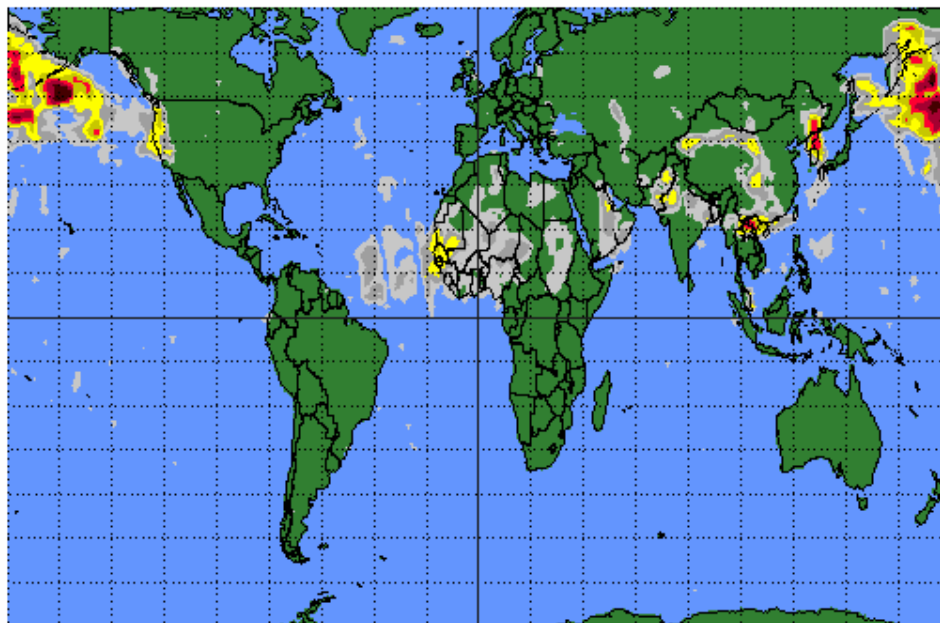


Figure 2-ii. TOMS Aerosol Index for April 12, 2001



Goddard Space
Flight Center

Figure 2-iii. TOMS Aerosol Index for April 13, 2001

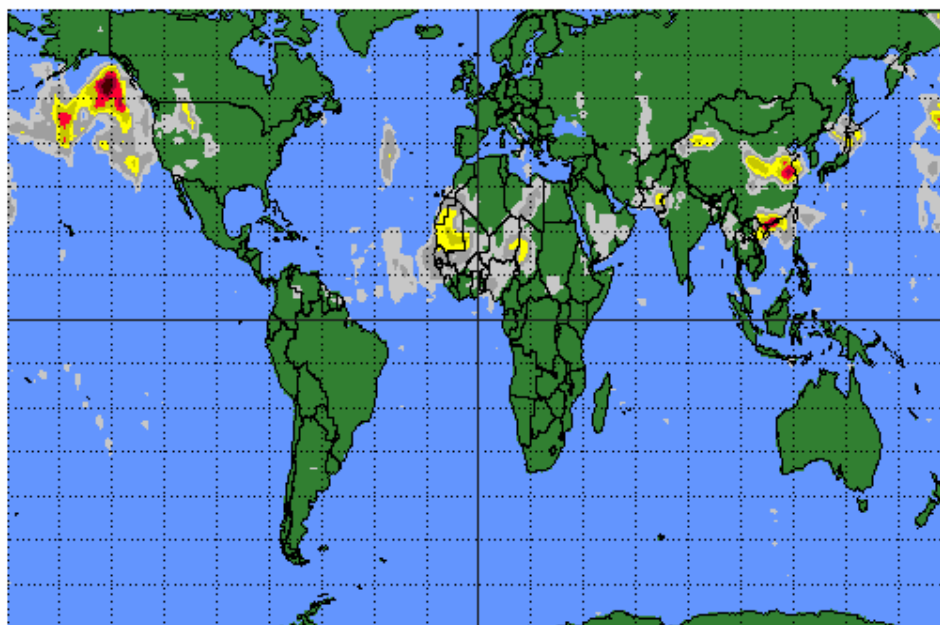
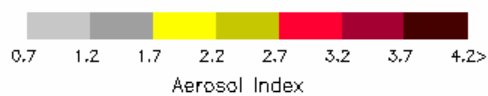
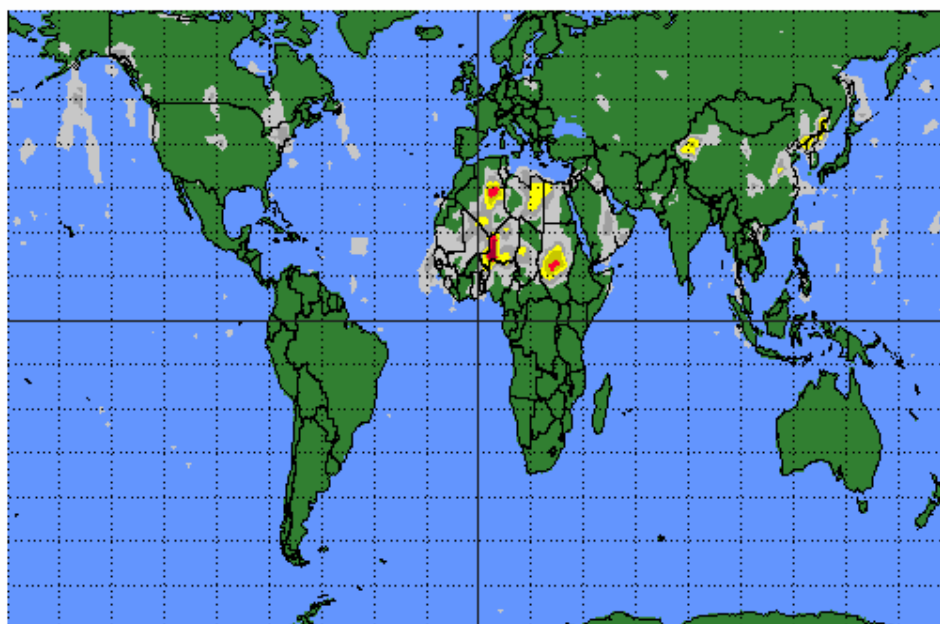


Figure 2-iv. TOMS Aerosol Index for April 16, 2001



Goddard Space
Flight Center

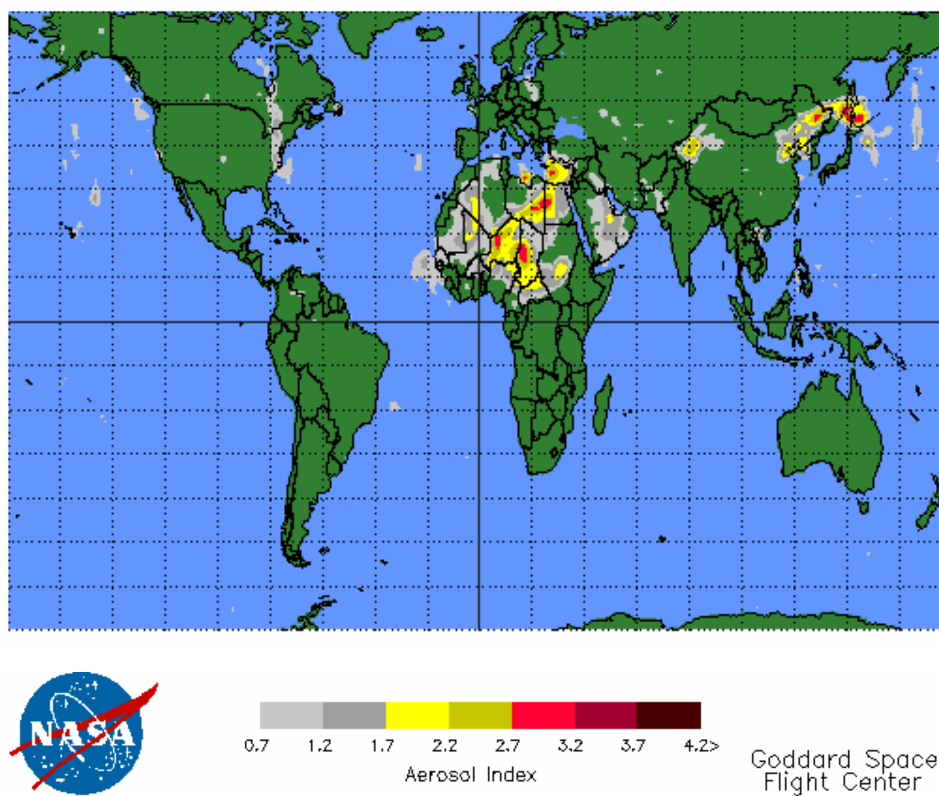
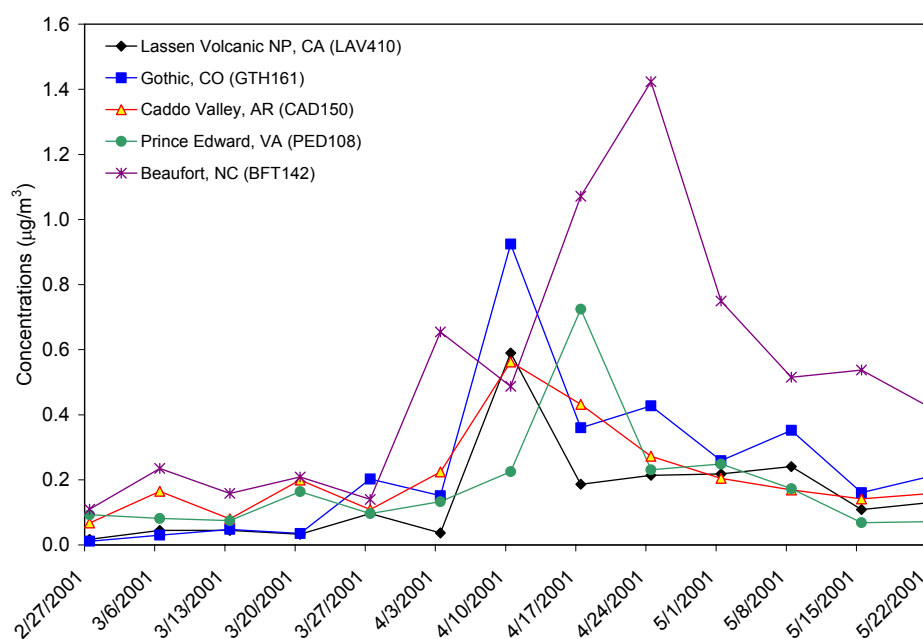
Figure 2-v. TOMS Aerosol Index for April 18, 2001**Figure 2-vi.** Time Series of Weekly Ca^{2+} Concentrations ($\mu\text{g}/\text{m}^3$)

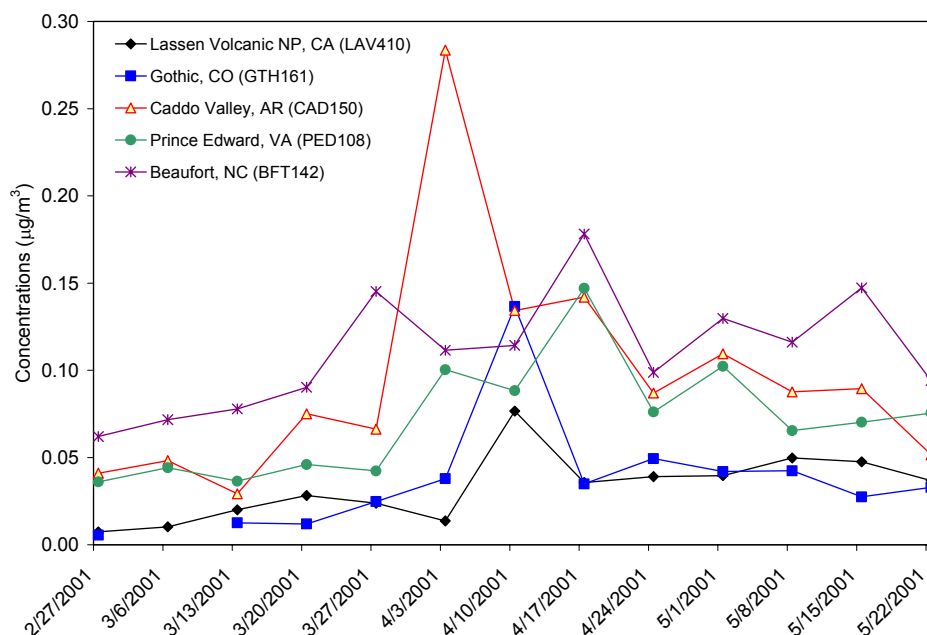
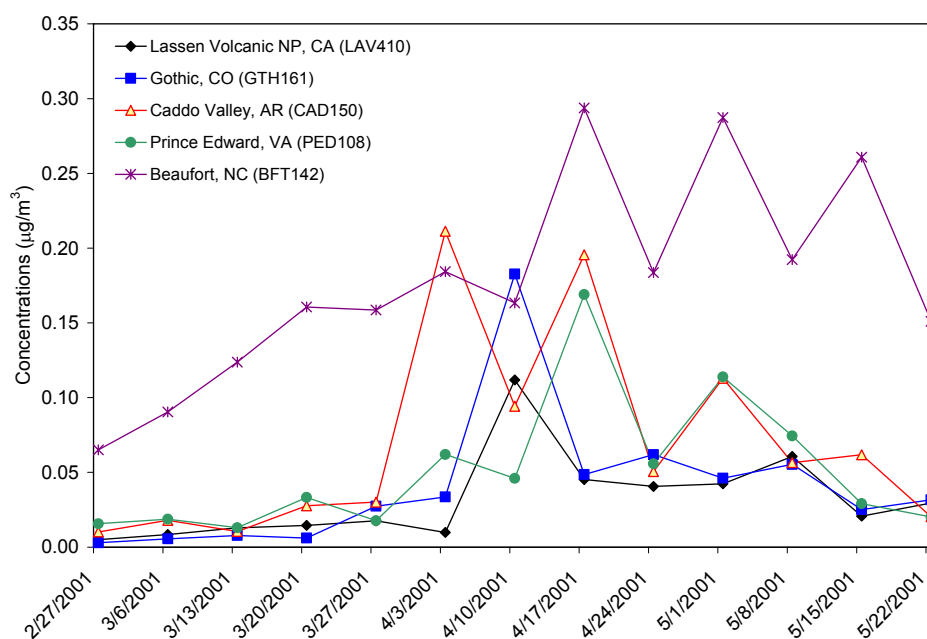
Figure 2-vii. Time Series of Weekly K^+ Concentrations ($\mu\text{g}/\text{m}^3$)**Figure 2-viii.** Time Series of Weekly Mg^{2+} Concentrations ($\mu\text{g}/\text{m}^3$)

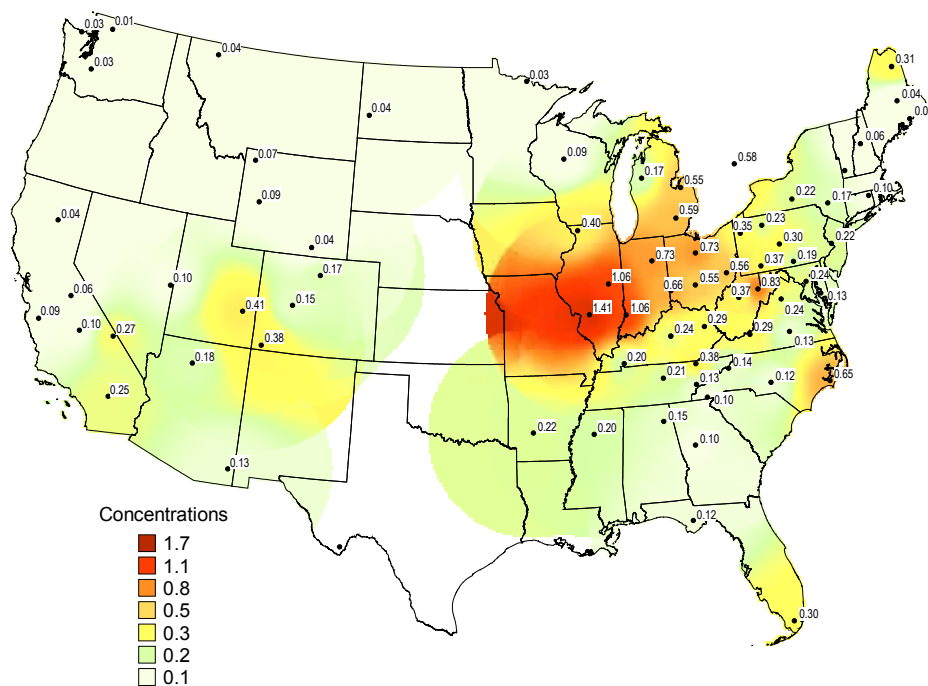
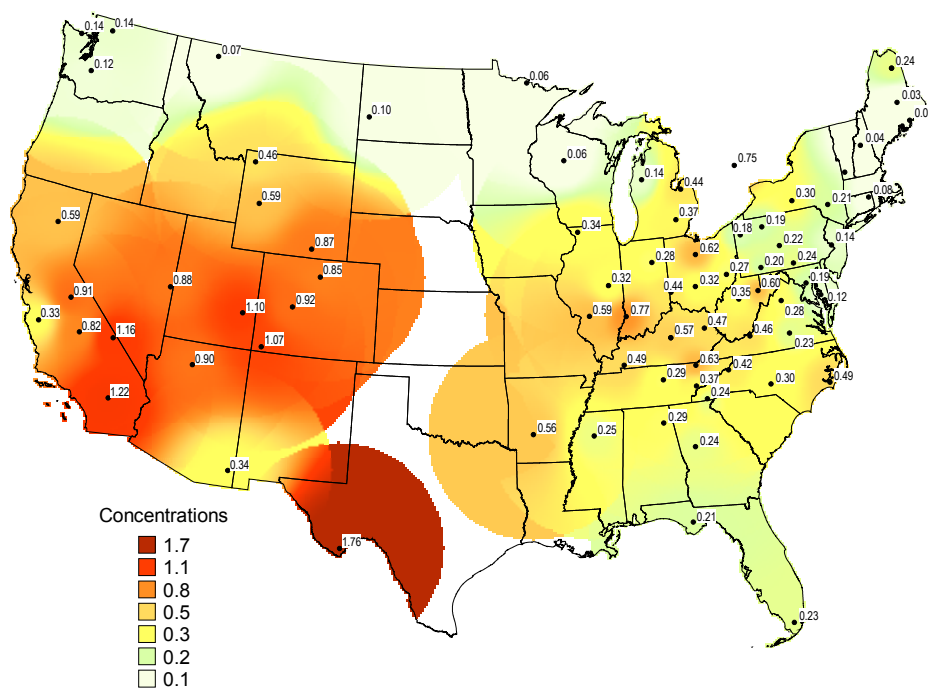
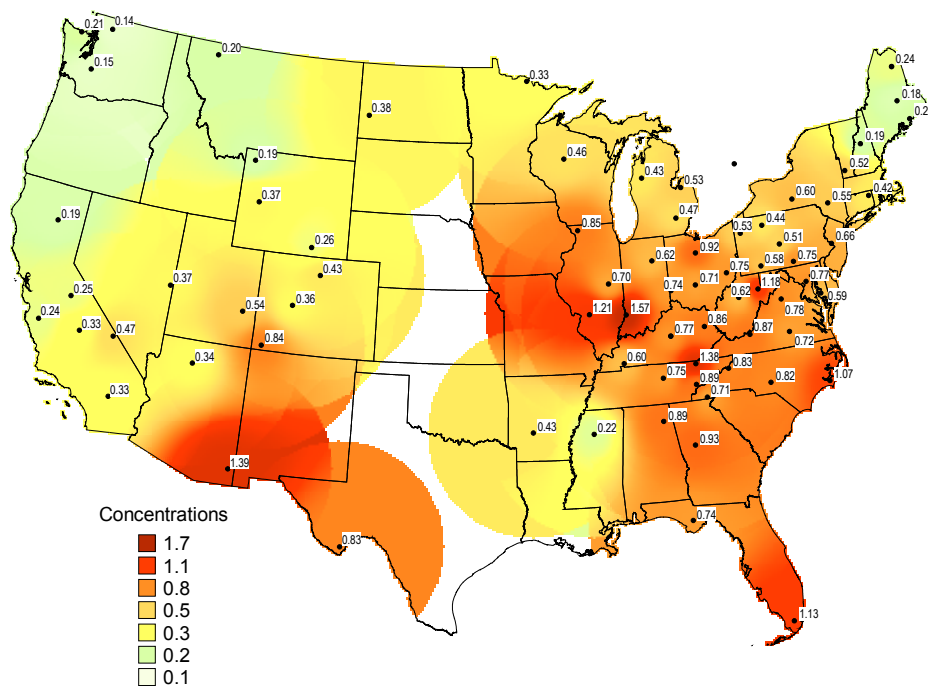
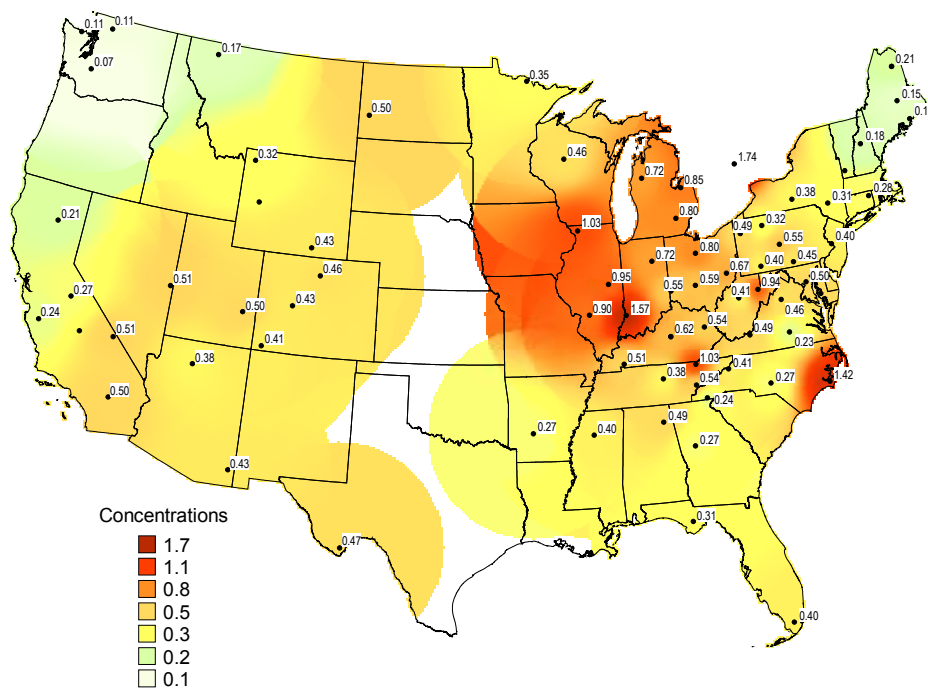
Figure 2-ix. Ca^{2+} Concentrations ($\mu\text{g}/\text{m}^3$) for the Week of April 3, 2001**Figure 2-x.** Ca^{2+} Concentrations ($\mu\text{g}/\text{m}^3$) for the Week of April 10, 2001

Figure 2-xi. Ca^{2+} Concentrations ($\mu\text{g}/\text{m}^3$) for the Week of April 17, 2001**Figure 2-xii.** Ca^{2+} Concentrations ($\mu\text{g}/\text{m}^3$) for the Week of April 24, 2001

This page intentionally left blank.